PERFORMANCE EVALUATION OF OFDM-NOMA IN MULTI-USER VISIBLE LIGHT COMMUNICATION

MASTER OF SCIENCE IN COMMUNICATION ENGINEERING AND NETWORKING

By

LIULE NEGASH BEYENE

HAWASSA UNIVERSITY

HAWASSA, ETHIOPIA

December 26, 2020

PERFORMANCE EVALUATION OF OFDM-NOMA IN MULTI-USER VISIBLE LIGHT COMMUNICATION

By

LIULE NEGASH BEYENE

A THESIS SUBMITTED TO THE SCHOOL OF ELECTRICAL AND COMPUTER ENGINEERING, INSTITUTTE OF TECHNOLOGY
SCHOOL OF GRADUATE STUDIES

HAWASSA UNIVERSITY

HAWASSA, ETHIOPIA

IN PARTIAL FULLFILLMENT OF THE REQUIREMENT FOR THE DEGREE OF MASTER OF SCIENCE IN COMMUNICATION ENGINEERING AND NETWORKING

HAWASSA UNIVERSITY

INSTITUTION OF TECHNOLOGY

DEPARTMENT OF ELECTRICAL AND COMPUTER ENGINEERING

SCHOOL OF GRADUATE STUDIES

ADVISORS' APPROVAL SHEET

This is to certify that the thesis entitled **"Performance Evaluation of OFDM-NOMA in Multi-User Visible Light Communication"** submitted in partial fulfillment of the requirement for the degree of Master's with specialization in Communication Engineering and Networking. The graduate of the Department of Electrical and Computer Engineering, and has been carried out by LIULE NEGASH, ID. No. PGComR/006/10, under my supervision. Therefore, I recommended that the student has fulfilled the requirements and hence hereby can submit the thesis to the department.

Advisor: **Dr.Zelalem Hailu (PhD)**

Signature: ______

Date: 26/10/2020

Co-Advisor: **Mr. Abriham Lule (MSc)**

Signature: ______

Date: ______

DECLARATION

I hereby declare that this thesis is my original work and has not been presented for a degree in any other university, and all sources of material used for this project have been duly acknowledged.

Student Name: **Liule Negash**

Signature: ______________________________

This MSC thesis has been submitted for examination with my approval thesis advisor's.

Advisor: **Dr. Zelalem Hailu (PhD)**

Signature: ______________________________

Co-Advisor: **Mr. Abriham Lule (MSc.)**

Signature: ______________________________

Hawassa, Ethiopia

Date of submission: October 14, 2020

Examiner's APPROVAL SHEET

SCHOOL OF GRADUATE STUDIES

HAWASSA UNIVERSITY EXAMINERS' APPROVAL SHEET

(Submission Sheet-2)

We, the undersigned, members of the Board of Examiners of the final open defense by Liule Negash Beyene have read and evaluated his/her thesis entitled "**Performance Evaluation of OFDM-NOMA in Multi-User Visible Light Communication**", and examined the candidate. This is, therefore, to certify that the thesis has been accepted in partial fulfillment of the requirements for the degree.

Dr. Zelalem Hailu		24/12/2020
Name of Major Advisor	Signature	Date
Name of Internal Examiner-I	Signature	Date
Name of Internal Examiner-II	Signature	Date
Dr. Mulugeta Mekonnen		
Name of External examiner	Signature	Date
SGS Approval	Signature	Date

Final approval and acceptance of the thesis is contingent upon the submission of the final copy of the thesis to the School of Graduate Studies (SGS) through the Department/School Graduate Committee (DGC/SGC) of the candidate's department.

Stamp of SGS Date: ____________

Remark

- Use this form to submit the thesis **with or without minor correction** suggested by the examining board
- 3 copies

ACKNOWLEDGEMENTS

Primarily, praises and thanks to the God, the Almighty, for His showers of blessings throughout my work to complete the thesis successfully. This thesis is finalized with prayer of numerous and love of my family and friends. However, few persons that I would like to particularly acknowledge and extend my heartfelt gratitude have made the completion of this thesis possible. With the biggest contribution to this thesis, I would like to thank my advisor **Dr. Zelalem Hailu (PhD)** had given me his full support in guiding me with inspiring suggestions and reassurance to go ahead in all the time of the thesis. I would also like to thank co-advisor **Mr. Abriham Lule (MSc)** for his kind support during this work. I am thankful to **Mr. Mesfin Fanuel,** Head of Electrical and Computer Engineering Department, for providing us with the adequate infrastructure in carrying the work. I am also thankful to **Mr. Fishum Zerifu** Coordinator, Communication stream department, for the motivation and inspiration that triggered me for the thesis.

Next, I would like grateful thank to School of Electrical and Computer Engineering staffs, especially for all Communication Engineering staff for their positive attitude to do this thesis.

Last but not the least, I would like to thank my family for giving birth to me at the first place and supporting me spiritually throughout my life and all the people who have supported me to complete the thesis work directly or indirectly.

ABSTRACT

Visible light communication (VLC) is a progressing green communication expertise for indoor wireless communication networks. Visible light communication (VLC) uses light emitting diodes (LEDs) for together lighting and communication. On non-orthogonal multiple access (NOMA) increases the system throughput by improving spectral efficiency. In indoor VLC networks, the gain ratio power allocation(GRPA) of NOMA assigns superior signal power to consumers of poor channels to succeed both fairness and high data rate. However, current GRPA approaches settled for radio frequency channels are not essentially active in all VLC channel and illumination circumstances. In this thesis, we start the resource allocation (RA) problematic on behalf of the downlink orthogonal frequency division multiplexing centered non-orthogonal multiple access (OFDM-NOMA) scheme to decrease the interfering amongst multi-users by applying cluster formation in the parameter of BER, sum rate maximization. After this thesis has done, the outcomes have to make low BER and high sum rate.

Key words: Visible light communication (VLC)**,** Non-orthogonal multiple access (NOMA), gain ratio power allocation (GRPA), orthogonal frequency division multiplexing (OFDM).

Table of Contents

LIST OF TABLES

LIST OF FIGURES

LIST OF ABBREVIATIONS

AP…......................................Access Point

AUDR……………………….Average User Data Rate

AWGN………………………Additive White Gaussian Noise

BER………………………….Bit Error Rate

BW…......................................Bandwidth

CD…......................................Code Domain

CDMA……………………….Code Division Multiple Access

CP……………………………Cyclic Prefix

CSI….......................................Channel State Information

DC……………………………Direct Current

DD……………………………Direct Detection

DCO-OFDM……………….…DC-Biased Optical Orthogonal Frequency Division Multiplexing

EAC…......................................Ergodicity and Comparison

EMI….......................................Electromagnetic Interference

EPA……………………………Enhanced Power Allocation

FFT…..Fast Fourier Transform

FOV……………………………Field of Views

FPA……………………………Fixed Power Allocation

GRPA………………………….Gain Ratio Power Allocation

5G…..Fifth Generation

IOT…..Internet of Things

IM………………………………Intensity Modulation

IFS…..Inter Frame Spacing

IF…..Infrared

IFFT…...Inverse Fast Fourier Transform

LD………………………………Laser Diode

LED…………………………….Light Emitting Diode

LOS…………………………….Line of Sight

MUI…………………………….Multi-User Interference

MUS…..Multi-User scheduling

MIMO……………………………….Multiple Input Multiple Output

NLOS…..Non-Line of Sight

NOMA……………………………….None Orthogonal Multiple Access

ONOMA…………………………….Optical None Orthogonal Multiple Access

OMA…………………………………Orthogonal Multiple Access

OFDMA….......................................Orthogonal Frequency Division Multiple Access

OWC…...Optical Wireless Communication

PD…………………………………….Power Domain

PD…………………………………….Photo-Detector

PF…………………………………….Proportional Fairness

PLS……………………………………Physical Layer Security

PTP……………………………………Peak-to-Peak

QAM………………………………….Quadrature Amplitude Modulation

RF……………………………………..Radio Frequency

RGB…..Red-Green-Blue

ROYGBIV…………………………….Red-Orange-Yellow-Green-Blue-Indigo-Violet

SC…………………………………….Super Position Coding

SIC……………………………………. Successive Interference Cancelation

SINR………………………………….Signal to Interference and Noise Ratio

SNR…...Signal to Noise Ratio

TDMA…...Time Division Multiple Access

UC-VT……………………………….User Centric Vectored Transmission

UE…………………………………….User Equipment

UV…………………………………….Ultra Violet

VLC………………………………….Visible Light Communication

Wi-Fi………………………………….Wireless Fidelity

CHAPTER ONE

1. INTRODUCTION

1.1. BACKGROUND

The explosive growing of linked devices, due to the emergence of Internet of Things (IoT) and the growing number of broadband mobile subscribers, lead to an unprecedented growth in traffic demand. In this respect, the next generation wireless networks are intended to come across this growth and offer new technical challenges to address the requirement for low latency and high spectrum efficiency. The continuing research struggles have mostly concentrated on two core directions. The first one is improving the spectral efficiency(SE) of the existing RF spectrum by embracing advanced modulation schemes, new multiple access techniques and efficient bandwidth use again; and the second one is discovering the abilities of the unlicensed spectrum, i.e., Infrared(IR) (300 GHz - 430 THz) and visible light communication spectrum (430 THz - 790 THz). In those context, VLC has come out as a promising smaller cell technology that can be linked to the existing super-fast fiber networks and composes an integral part of the 5G communication systems [1].

A VLC system utilizes off-the-shelf standard LEDs to enable high-speed data transmission and, simultaneously, to offer indoor/outdoor illumination. It can be recognized by modifying and demodulating the light intensity of the light emitting diodes (LEDs) in a procedure known as intensity modulation/direct detection (IM/DD). The greatest nice-looking types of VLC are the typical communication security, the high grades of spatial recycle, and its invulnerability to RF interfering, which concentrates safe for action in environments through high electromagnetic interference (EMI), such as hospitals and industrial plants. Because the commercial LEDs are designed only for lighting systems, we need an effort to enhance the modulation characteristic of LEDs. When the area of LED is greater in amount, integral junction capacitance of LEDs is also become bigger depending on the area of LEDs and then resistance- capacitance (RC) delay time of LEDs is increased. As a result, the modulation bandwidth is limited by large resistance-capacitance (RC) delay time. Furthermore, visible light cannot enter through furthermost objects and walls, creating it well matched for small cell design and capable of provided that high quality service area without inter-cell interference. This constitutes visible light communication (VLC) a viable gorgeous technology and an operative complement to current radio frequency (RF) communications[2].

In spite of its great benefits, VLC systems have definite shortcomings which want to be fully addressed so as to exploit the full capacities of this emerging technology. A key drawback of VLC systems is that the attainable data rates are limited to the restricted modulation bandwidth of the LEDs, which periods few MHz Therefore, in order to recognize the envisioned VLC systems with full abilities, there has been enlarged interest in the efficient development of advanced optical modulation techniques, optical MIMO and multiple access schemes[3].

As a technology enabler for 5G networks and elsewhere, VLC is intended to offer ubiquitous connectivity and high spectral efficiency. To this termination, numerous optical (orthogonal and non-orthogonal) multiple access schemes have been planned in the open literature, addressing these challenges. In OMA, dissimilar users are allotted to orthogonal resources in either the frequency or time domain. For instance, OFDMA allocates unlike frequency sub-carriers to diverse users, whereas TDMA permits users to share the identical frequency by accessing the network in a quick succession during their allotted time slots[4]. On the contrary, NOMA permits multiple users to concurrently utilize the entire existing frequency and time resources, leading to greater enhancements in spectral efficiency associated to OMA schemes. NOMA can be realized through two dissimilar attitudes, namely, PD NOMA and CD NOMA. In PD NOMA, customers are multiplexed in the power domain by allocating distinctive power levels to dissimilar users, while CD NOMA make use of user-specific spreading sequences in order to multiplex the users in the code domain similarly to the well-known CDMA technique[5].

It is worth noting which PD NOMA has been seen to be predominantly appropriate for VLC downlink (DL) systems for numerous reasons. First, PD NOMA is frequently used to multiplex a small number of numbers of customers, which is in-line with the desires of VLC systems that address LEDs as small cells to serve a small number of users. Second, power allocation in PD NOMA is fully dependent on the channel gain obtainable at or channel state information the transmitter, and channel approximation in VLC is noticeably less error-prone, compared to RF, due to the time-invariant channel gain those remainders continuous till the location of the receiving station variations. Because VLC does not interfere with electronic devises as RF waves do. Therefore, VLC more suitable for applications where sensitive electronics devises are used, such as hospitals, chemical plant and airplane. Third, PD NOMA achieves better in high SNR scenarios, which is the situation in VLC systems due to the strong LOS channel gain and the short separation between the communication front ends. Lastly, the performance of PD NOMA systems can be developed by enhancing the channel gain dissimilarities between users, which can be attained by tuning the transmission angles of the LEDs and the field-of-views (FOVs) of the PDs, proposing two degrees of freedom to optimize the system performance. Hence, the thesis focus to PD NOMA in VLC[6].

1.2. STATEMENT OF THE PROBLEM

Optical wireless communication, particularly visible light communication (VLC), is becoming a promising candidate to tackle the problem of spectrum looming in the conventional RF based wireless communication. There is a huge interest towards VLC due to the possibility of using the lighting infrastructure for both illumination and high speed connectivity at the same time. The main goal of this thesis is to find the optimal user center vector transfer (UC-VT) cluster formation for maximizing the sum rate by making different groups, while scheduling UEs in a proportional fairness (PF) manner, which is ultimately a joint cluster formation and multi user scheduling (MUS) problem. When the number of users increases the NOMA interference problem is appeared. The interference of the power- domain NOMA can be reduced by successive interference cancellation when power- domain NOMA and OFDM schemes are combined. In order to diminish the performance deprivation forced by the Interference, a User-Centric (UC) cluster establishment procedure is scheduled for the VLC down-link system, where multiple customers are concurrently held by multiple Access Points (APs). In this thesis there is multi user interference and computational problems among multi users in visible light communications. These problems can be solved by clustering users in to separate groups based on their respective channel gains and implementing OFDM-NOMA on those separate groups.

1.3. OBJECTIVES OF THIS THESIS

1.3.1. General Objective

The main objective of this thesis is to analyze and evaluat the performance of OFDM- NOMA in multi user visible light communication problems by clustering users in to separate groups based on their own channel gains and realizing NOMA on those separate groups.

1.3.2. Specific Objectives

- To model the mathematical or analytical framework of user clustered OFDM-NOMA multiple accesses for visible light communication based on channel state information (channel gain) based user clustering.
- To analyze the performance OFDM-NOMA based multiple accesses schemes.
- To evaluate the performance of OFDM-NOMA in visible light communication

.

1.5. **LITERATURE REVIEW**

In [1], the authors have studied the optimal beam steering parameters for VLC when there are more users than the steerable components. They have found the optimal steering angles and LED directivity for a single LED and multiple users. The outcomes display that steering VLC beams and altering the directivity can recover the user rates significantly. This research did not concern the interference among multi-users. It only considers the directivity of the beam steering.

In [2] the complicated mathematical forms in the NOMA-VLC throughput, this paper presented an alternative bound to facilitate the comparison of GRPA strategies. The compactness between the alternate bound and actual capability was studied using both analytic and numerical outcomes. For the ceiling-illumination case, they are demonstrated that their IFS approach is better than PLS with respect to AUDR. For the workbench-illumination case, the paper gives the necessary conditions that are needed for their IFS approach to remain better.

In [3], the authors have demonstrated the trade-off between capacity and reliability, from their task the performance of a two-user scenario for both O-NOMA and OFDMA. They have shown the normalized system throughput and the error rate performance, respectively. Both multiple access systems are based on DCO-OFDM transmission with a lesser channel state information. Here O-NOMA provides a significant upgrading in the overall method throughput compared to OFDMA. However, the detected throughput improvements provided by O-NOMA come at the payment of performance loss in link dependability.

In [4], the authors have proposed a simple user grouping and pairing scheme for non- orthogonal multiple accesses in a downlink visible light communication system. The proposed scheme is a mix of both conventional non-orthogonal multiple access and the conventional orthogonal multiple access schemes. In the proposed system, every two handlers are paired using NOMA and all pairs are assigned with conventional OMA. The performance of the planned scheme is equated to the conventional OMA in terms of the maximum sum rate. The Simulation result has shown that the proposed scheme increases the capacity gain of the system compared to the OMA scheme. Furthermore, coupling users with a high dissimilarity in their horizontal distances would be increased the sum rate of the system. The gap of this paper is considering a simple user grouping and pairing scheme is proposed for NOMA and is applied for the downlink visible light communication (VLC) system. It did not consider multi users, which has interference.

In [5], the authors have investigated the sum-rate maximization problem in a downlink NOMA-based VLC system using optimal and computationally efficient sum-rate optimization techniques, while considering the user fairness and unique intensity constraints. The simulation results show that optimized NOMA-based VLC system outperforms the conventional NOMA-based VLC system in BER and sum rate in both cases.

In many literatures different variants of multiple access (MAC) schemes such as O-FDMA, OOFDM-IDMA, SC-FDMA, O-CDMA, and NOMA have been proposed for VLC. Among those schemes, NOMA is state-of-the-art (advanced) multiple access schemes, which have shown relatively good performance. However, NOMA experiences the following major challenges. These challenges of NOMA are: a) significant latency and intensive computational requirement for the case of large number of users b) If the channel gains of two or more users are nearly equal, NOMA will introduce high BER due to significant amount of interference from the signal intended to the neighbor users.

In [6] the combination of OFDM and NOMA were applied to VLC over offline demos, and displayed larger scheme throughput than that of the conventional OFDM. Nevertheless, the system is less appropriate for real-world applications under dynamic and various channel conditions, as static parameter loading is expected. Furthermore, subcarrier allocation is essential for system performance optimization, particularly when seeing different power fading conditions over every subcarrier/user in the bandwidth-limited VLC scheme.so, it is greatly required that the software-reconfiguration can be maintained in real-time to dynamically handle parameters such as power ratio and subcarrier number, in order to recognize elastic system capacity and manage resource allocation to user demand in OFDM-NOMA based VLC systems.

The customer with a poorer channel condition, represented as UE1, needs a larger power. A small power is assigned to the consumer with a good channel condition ,represented as UE2.Note that three different cases might arise due to the probability that the number of the assigned subcarrier of UE1 may be larger/smaller than or equal to that of UE2. When the similar numbers of subcarriers are chosen to UE1 and UE2, the resultant NOMA constellation, which is the overlapped signal of UE1 and UE2, would be a 16-QAM-like constellation. The added two cases will outcome in a 20-QAM-like constellation. In order to mend the users' information, the SIC technique is used to solve multi-user interference (MUI). Namely, at the receiver of UE1, the recovered signal is directly de-modulated, while the interference from UE2 is treated as noise.

Nevertheless, at the receiver of UE2, the signal constituent of UE1 is initially decoded. Consequently, the wanted signal of UE2 can be decoded by subtracting the signal component of UE1. In the cases that some subcarriers are assigned to one user only, there is no MUI over these subcarriers. Therefore, the proposed real-time dynamic power-and-subcarrier allocation order is a flexible solution for practical OFDM-NOMA system to fulfill the QoS requirements among users, as well as to ensure better user fairness. The authors proposed scheme, provides a flexible solution for multi-user VLC system to ensure better user fairness and fulfill different capacity demands.

In[7] the conventional multiple access, dissimilar users are allotted orthogonal resources in terms of time, code or frequency domains. The performances of VLC in these orthogonal schemes have been valued. Nevertheless, these orthogonal procedures cannot make optimal use of the resources. Since the data traffic is assumed to increase enormously from year to year, there is an occurrence to find out more efficient multiple access technologies become very important. Non-orthogonal multiple access (NOMA) has lately fascinated major consideration, which offers a higher spectral efficiency by allowing multiple consumers to share the similar time and frequency resource.

In practical VLC systems, compared to the receiver amplifier noise and background noise of the electrical circuit, the signal-dependent shot noise is negligible. Therefore, in this work, the authors assume the noise in the VLC system is Gaussian and signal-independent, and the Shannon formula, which has been widely applied in VLC is used to characterize the capacity of a VLC link with both LOS and non-LOS components taken into account. This research studies the power control problem for an OFDM-NOMA VLC system with arbitrary number of multiplexed users. The goal is to maximize system's sum rate with any given required SINR of each user. Based on theoretical derivations of the closed form of the optimal power ratio for the multiplexed users, an efficient EPA algorithm is proposed to realize both user- and subcarrier-level power allocation, and so maximizing the attainable sum rate of OFDM-NOMA VLC. Numerical results show that, in terms of sum rate and subcarrier loss rate, the proposed EPA algorithm exhibits significant performance improvement compared to the optimized FPA strategy and the conventional GRPA scheme.

In [9] due to the limitation of LED's bandwidth, OFDM is used to enhance the transmission capacity of VLC system. NOMA can support multiple customers in VLC scheme by sharing time and spectrum assets. Being an improvement of OMA technique, NOMA can be combined with OFDM to further increase the spectral efficiency. The OFDM-NOMA scheme has been studied intensively, which can improve significantly the overall transmission capacity of VLC system. In such a system, the intensity of modulated light has a large PTP value. At the receiver, the overall intensity of received signal is with an increased PTP value for multiuser VLC system, compared with the single-user VLC system. For the procedure of photo-detection, when the incident optical power is too high, some of the received signal with high power will be clipped, which leads to severe signal distortion and performance deterioration. Therefore, the adverse effect of peak clipping cannot be neglected when studying the OFDM-NOMA VLC system performance. In this paper, they propose a novel method to decode the multiple users' signals from the superposed signal, where high order M-QAM signals are used. This decoding method is called EAC. Different from SIC method; the EAC method can recover the signals for multiple users simultaneously, instead of decoding them one by one. Based on this, the authors study the BER performance improvement of OFDM-NOMA VLC system. Three modulation formats are considered, including 4-QAM, 16-QAM, and 64-QAM. The simulation results illustrate that the OFDM-NOMA VLC system performance is improved significantly by using the EAC method.

At the transmitter, Hermitian symmetry is used to guarantee the real output of OFDM signal. Therefore, only half of the spectrum is used to transmit the information. At the receiver, if the PTP value of optical signal is large, peak clipping occurs due to the nonlinear transfer characteristic of PD. In this paper, the author investigates the performance of two-user OFDM-NOMA VLC system. The traditional SIC decoding method does not work well for the signals with high order modulation formats. To improve the performance of OFDM-NOMA VLC system, the researcher proposed a novel decoding method, which is called EAC. The simulation outcomes indicate which the proposed EAC method can provide better BER performance than the SIC method, when high order M-QAM ($M > 4$) signals are applied to the two users.

In [10] there are multiple access techniques, which are closely related to NOMA, including pattern division multiple access (PDMA) and spatial division multiple access (SDMA).PDMA can be realized in various domains. At the transmitter sideways, PDMA first maximizes the diversity and minimizes the overlays among multiple customers in order to plan non-orthogonal patterns. The multiplexing is formerly accomplished in either the code domain or spatial domain, or a combination of them. For SDMA, the working principle is stimulated by basic CDMA systems. Instead of using user-specific scattering orders, SDMA differentiates altered users by using user-specific channel impulse responses (CIRs). In this paper, the Categories of NOMA schemes are expressed in the following diagram.

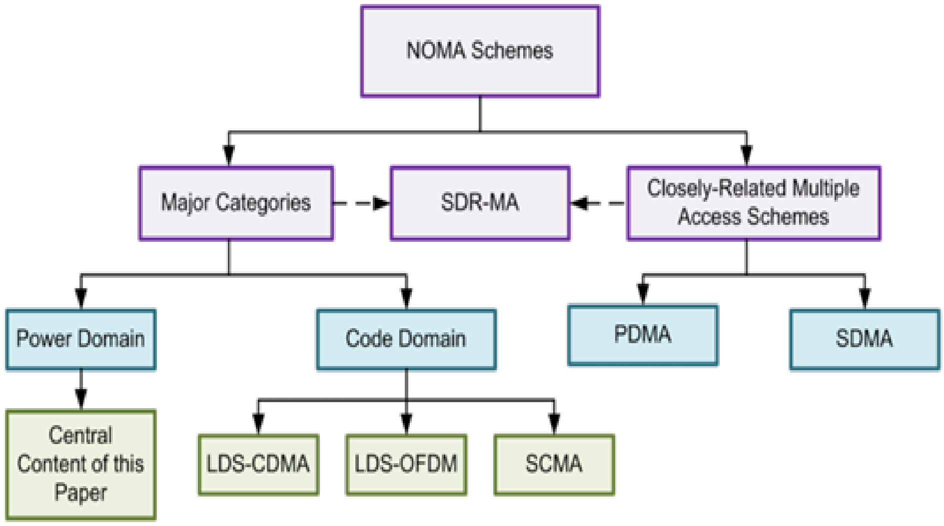

Figure 1.1 A simple classification of NOMA techniques

1.6. SCOPE OF THE THESIS

This thesis is confined to reduced bit error rate among multiple users based on OFDM-NOMA, which introduces a performance evaluation of multi user visible light communication for the case of N number of users, when N=1-12. If the channel gains of two or more users are nearly equal, NOMA will introduce high BER due to significant amount of interference from the signal intended to the neighbor users. The interference is reduced by clustering users in to separate groups based on their respective channel gains and implementing NOMA on those separate groups.

1.7. METHODOLOGY

The following activities are expected for the execution of this thesis.

Literature review (study):-In the literature review we have revised, many journals related to the thesis that we implement to solve the problems of interference among multi-users. Some of the revised works are mentioned in this thesis with their outcomes.

System design: Design to detail the block diagram and described each OFDM-NOMA in VLC

Using MATLAB:-The mathematical equations we write the mat lab program to show the BER, interference and latency based on the multi-users clustered on OFDM-NOMA using mat lab numerical simulations.

Result and Discussion:-Based on the mat lab simulation, we discuss the result what looks like. Based on these results on the BER and sum rate and interference values would be discussed.

Final report:-Finally, the whole works what we have done, would be reported to the concerning person who evaluate it.

CHAPTER TWO

2. OPTICAL WIRELESS COMMUNICATION (OWC)

In the past years, the wireless technology had spread broadly. One of the greatest essential reasons lies in the necessity of persons to stay always linked at high speed to the network. Whether for work or for enjoyable more and more people have the constraint to be connected in any position at high speed. Besides, with the growth of web technology the amount of transmitted data increased extremely[11].

Humankind has been using light as a communication medium for numerous years, and light continues to be of excessive advantage in the area of communication. Fire had been used to made smoke signals on clouds; which is a kind of visual communication. After the discovery of the electric light bulb by Thomas Alva Edison in the 19th century, new ways were established to use light to communicate. The origination of the electric bulb LED to the origination of the Signal Lamp, a visual signaling method used for optical communication developed by Arthur C. W. Aldis. Stereotypically, the Signal Lamp uses Morse code to provide information to the viewer by making shutters mounted on the front of the lamp open and close [6].

The impression of using light as a communication medium was realized by Alexander Graham Bell in 1880 with his discovery of the photo phone, a device that transmitted a voice signal on a beam of light. Bell concentrated sunlight with a mirror and then spoke into a mechanism that shook the mirror. The detector at the receiving termination picked up the vibrant beam and decoded back into the voice signal, the similar process as the phone did with electrical signals. Nevertheless, Bell could not generate a beneficial carrier frequency, nor was he able to transfer the light beam from point to point. Obstacles in nature such as fog and rain that could interfere with the photo phone made Bell stop any future[12]

Until today, a radio frequency-based technology has been able to see these requirements, but in the next future, there will be a problem: the volume of transmitted data increases exponentially but the radiofrequency band is limited. A possible result to this problematic is the optical wireless technology. Optical wireless technologies are fresh communication technologies where the info is transported through modified beams of visible light or infrared light. OWC has different properties with respect to radiofrequency transmission[13].

Table 1 Radio – OWC comparison [7].

No	property	Radio	Optical wireless
1	Bandwidth regulated	Yes	No
2	Pass through opaque object	Yes	No
3	Multipath fading	Yes	No
4	Multipath propagation	Yes	Yes
5	Path loss	High	High
6	Input X(t)represents	Amplitude	Power

As one can see from table 1 the main benefit of OWC with respect to radio communications is that the OWC is not regulated, the entire OWC bandwidth is free and not licensed. That is a prominent benefit for anybody that would plan and commercialize OWC methods.

Table 2. Radio-VLC comparison.

Radio bandwidth	VLC bandwidth(table 2.2.1)	$Ratio: \frac{VLC}{Radio}$
Band ≈ 300GHz	Band=869THz-400THz $\approx 470THz$	$\frac{490THz}{300GHz} = \frac{490*10^3 GHz}{300GHz} \approx 1600$

From table2, the VLC bandwidth is approximately 1600 times wider than the radio Bandwidth. OWC, in a different way from radio, does not pass through opaque things. This is an advantage in terms of security for the reason that the signal can be limited to a confined area. Another benefit is that OWC does not hurt from multipath fading that is the attenuation of the signal due to reflections and refractions. The latter difference from radio is which the communication in OWC is based on the wave power and not on the amplitude of the electromagnetic field. Therefore, in OWC, the estimated signal can be only positive in the meantime; in radio signal, the signal can be positive or negative. The remaining properties in table 1 are in communal: both radio and optical waves hurt from multipath distortion due to reflection of the signal; furthermore, the path loss in which for OWC is proportional to distance square as in radio communications deals.

2.1. VISIBLE LIGHT COMMUNICATION

Visible light communications (VLC) is a subdivision of optical wireless communication (OWC) that contains electromagnetic waves in the visible spectrum. Many VLC communication applications that are defined in the following are valid for OWC methods and vice versa. As stated above VLC is a subset of OWC that uses visible light spectrum to communicate. With regard to OWC, VLC applications through only the visible spectrum and not the infrared or ultraviolet spectrum. In general, VLC use commercial LEDs to communicate. LEDs have a wide white wavelength emission spectrum, which encompasses all the visible light. This may seem as a very limiting simplification however in practice, it is not, because, thanks to the receiver photodiode and lenses filter, one can study the transmitter light as a sum of many single monochromatic waves.

OWC usages light waves to transmit and receive information, and the benefits of OWC will be fast communication speediness and the circumstance that users do not have to pay to use the light spectrum.

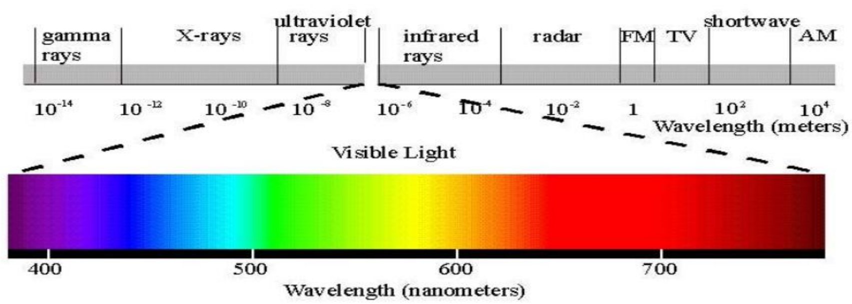

Figure 2.1 Visible Light Spectrums [9]

OWC covers the entire light spectrum, and VLC belongs to OWC using the Visible Light spectrum. The Smart Bulb is a successful example of VLC. Using the smart bulbs, people can easily manage all bulbs in a room. However, most VLC systems require installing new equipment. In the case of the Smart Bulb, if we want to construct the VLC system in a room, it is required to replace all bulbs to smart bulbs designed for VLC[14].

2.1.1. Involved frequencies

All transmission systems use waves to communicate. In particular, radio and optical communication use electromagnetic waves to transport information. The electromagnetic spectrum is very wide and is classified by wavelength or by frequency. These measures are closely linked by the formula:

$$\lambda = \frac{c}{f} \qquad \ldots\ldots\ldots\ldots\ldots\ldots\ldots\ldots\ldots\ldots 2.1$$

Where c is the speediness of light λ is the wavelength and f is the frequency.

The VLC electromagnetic spectrum is in general classified in wavelength intervals that match approximately to colors perceived by the human eye as shown in table 3.

Table 3 OWC waves' classification and value

Color	Frequency(THz)	Wavelength(nm)	Type
Ultraviolet(near UV)	789-869	300-380	OWC
Violet	668-789	380-450	VLC
Blue	631-668	450-475	VLC
Cyan	606-631	476-495	VLC
Green	526-606	495-570	VLC
Yellow	508-526	570-590	VLC
Orange	484-508	590-620	VLC
Red	400-484	620-750	VLC
Infrared (Near IR)	400-214	750-1400	OWC

2.1.2. Flickering

Flickering is a fast variation of the intensity of the source. This phenomenon always exists in visible light communication (VLC) light sources because the transmission technique uses intensity variants to transmit the signal. However flickering represents a light flashing which is perceivable from human eyes and causes distress. The flickering is perceptible from humans when the light source does not meet definite situations. Flickering is characterized by manageable factors like the light bulb blink frequency or the illumination intensity variant and uncontrollable factors like the people gradation of light/dark adaptation, the age and fatigue[15].

2.1.3. Intensity Modulation – Direct Detection (IM-DD)

In general, two methods of VLC transmission/detection are possible: intensity modulation direct detection IM-DC and coherent transmission/detection.

The coherent transmission/detection is often related with laser diodes (LD). The IM-DD instead is related through light emitting diodes (LED). This scheme is used because the LED, unless one uses complex and costly methods, cannot create coherent waves. IM-DD is a transmission system in that the intensity of the optical source is modified by the signal, and the demodulation is attained through direct detection of the optical carrier and change using a photo-detector. This work gives the IM-DD and does not study the coherent transmission/detection. The IM-DD VLC schemes are low-priced and easiest to implement and the lasers on the other sideways are risky for human eyes. This is the reason that leads to consider LED IM-DD for commercial daily applications[16].

Similar to other wireless optical communication systems, VLC relies on intensity modulation and direct detection (IM/DD) for data transmission.

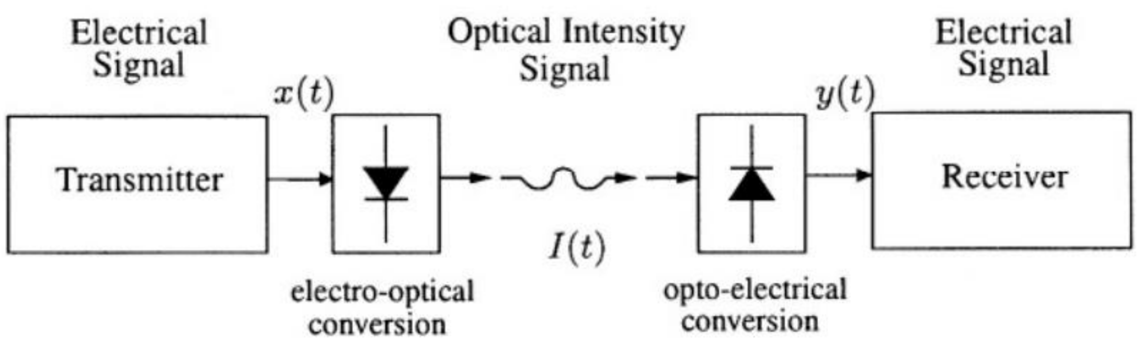

Figure 2.2 A block diagram of an intensity modulated direct detection channel [10]

Figure 2.2 displays a block diagram of an intensity modulated direct detection system. The instantaneous optical intensity $I(t)$is modulated proportional to the input electrical current$x(t)$.This method of modulation is termed as intensity modulation and can be done by a laser diode (LD) or a light emitting diode (LED). Usually, LEDs have higher reliability, lower cost and are considered more eye safe compared to laser diodes is their higher speed of operation.

After data modulation, the intensity signal is transmitted through the channel .At the receiver, a photo diode is used to detect the received intensity .This method of detection is termed as direct detection.

2.1.4. Photodiodes

Photodiodes are solid-state device that are used to perform that optical to electrical conversion. They create the output electrical current $y(t)$, proportional to the expected intensity signal. The received current is then processed to extract the transmitted information. The key parameter in photodiode is the responsivity defined as,

$$R = \frac{I_p}{P_p} \qquad \text{2.2}$$

Where, I_p is the average photo current generated and P_p is incident optical power .The photodiode responsivity depends on the physical structure of the photodiode and has the units of ampere per watt. Two shared photodiodes, which are currently used in practice, are p-i-n photodiodes and avalanche photodiodes. The first kind has lesser cost but lower modulation bandwidth. The received power of the photodiode P_p is proportional to its effective light collection area. Therefore, the photodiode effective area must be huge sufficient to gather the transmitted signal. In general, photodiodes must be selected such that the cost, performance and safety requirements are satisfied[17].

2.1.5. LED Characterization

In this study, the work is concentrated on the semiconductors formed by P-type and N-type materials. LED is a PN junction semiconductor, which radiates light when frontward biased releases the energy in the form of photons. This effect is called as electroluminescence. What makes LED different from other diodes? It is the band gap of the LED that is designed for radiative recombination.

When linking the N-type and P-type resources, the Fermi levels (W_f) will be allied and will yield an energy barrier even when there is no exterior voltage applied. There are two energy bands, namely the conduction band and valence band that are detached by a forbidden region through the width of Wg. In the conduction band, electrons not bound to singular atoms are free to travel. In the valence band, boundless holes are mobile that have positive charge. The free electrons in the N region cannot go up the barrier without the external energy; that is the same for the holes that cannot surmount the barrier. By applying a adequate energy (eV), a free electron crosses the barrier, drops into the inferior energy level and recombines with the hole, releasing the energy in the form of photons[12].

A light-emitting diode (LED) is a semiconductor that have light source. Two useful lighting aspects of LEDs are color rendering index and luminous efficacy. The color-rendering index is a degree of the ability of the LED to harvest color in contrast with an ideal light source. The luminous efficacy on the other hand, is the degree of the effectiveness with that the source yields visible light from electricity. It is equal to the ratio of luminous flux, defined in the total electric power consumed by the source[17].

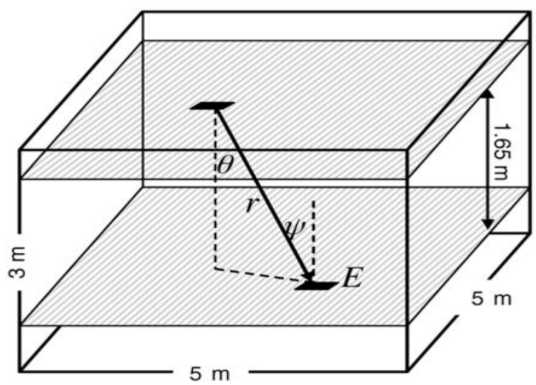

Figure 2.3 An indoor application of visible light communications [10]

Consequently, it has the units of lumen per watt ($\frac{lm}{w}$).

2.2. White Light Emitting Diodes

Although every single color can be created by LEDs within the visible expanse, white light is the most required color for general illumination. The visible radiation measurable to the human eye is between 480nm to 750nm. White light emission from an LED is by combination of multi-color LEDs or by the combination of phosphors with blue/UV LED emission. There are different kinds of white LEDs. Some of the essential ones are[12]:

2.2.1. Phosphor based White LEDs

The InGaN blue LED is coated with phosphor. The wavelength changing phosphors is joined with a blue LED to emit white light. The chip inside the LED emits blue light while exterior voltage is applied. The emitted blue light permits through the yellow phosphor, yielding white light emission.

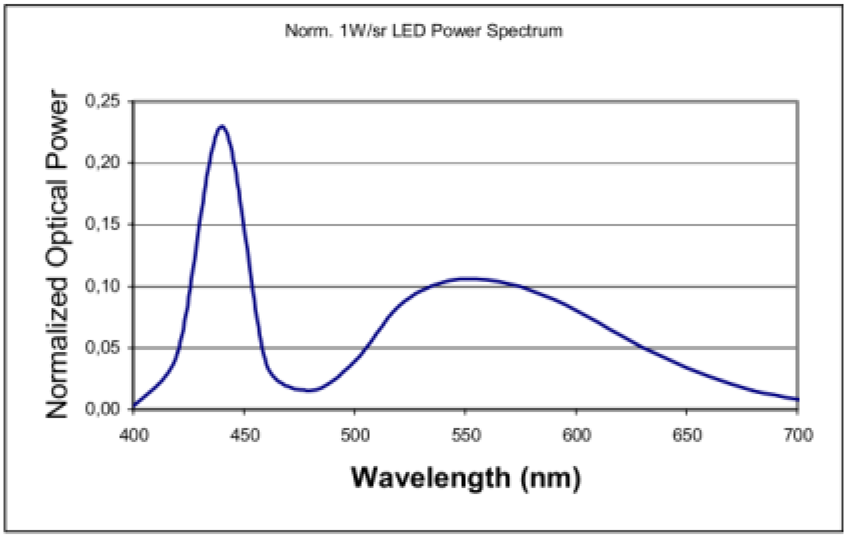

Figure 2.4 Normalized optical spectrum of a white LED [7]

2.2.2. Ultraviolet (UV) based White LEDs

Ultraviolet LEDs were made-up with pre-coating blue/green/red phosphors onto ultraviolet (UV) LED to produce white light.

2.2.3. RGB (Red-Green-Blue) LEDs

An RGB (red, green, blue) 3-chip LED is a mix combination of three colors to yield white light with tiny variance in the Kelvin color temperature. What we get coming from the sun is white light. We see that the visible spectrum of radiation which the sun releases is truly a wide range of wavelengths, extending from red to orange, yellow, green, and blue, indigo to violet (ROYGBIV). While this wide range of colors impinges on our retina, our brain interprets it as "white". A tri-color LED attempts to mimic this result by outputting a wide range of wavelengths (red, green and blue). Note that the three dominant wavelengths of the tri-color LED are at the ends and the middle of the visible spectrum, therefore attempting to reproduce the coverage of the range and receiving close to (ROYGBIV) as possible (with minimal hardware). Therefore, it is less of a mixing and more of an attempt to create a continuous function by using a few sampled points.

2.3. **Working principle of VLC technology**

All the data from internet is streamed in to the lamp driver. VLC is implemented using LED light bulbs at downlink transmitter. By fast variation of current, optical output can be made to differ at enormously high speed. An overhead lamp fitted with LED with signal processing technology streams data embedded in its beams at ultra-high speeds to the photodiodes. A receiver dongle then changes the small channels in amplitude in to electrical signals, which is then converted back in to a data stream and transmitted to a computer and mobile device.

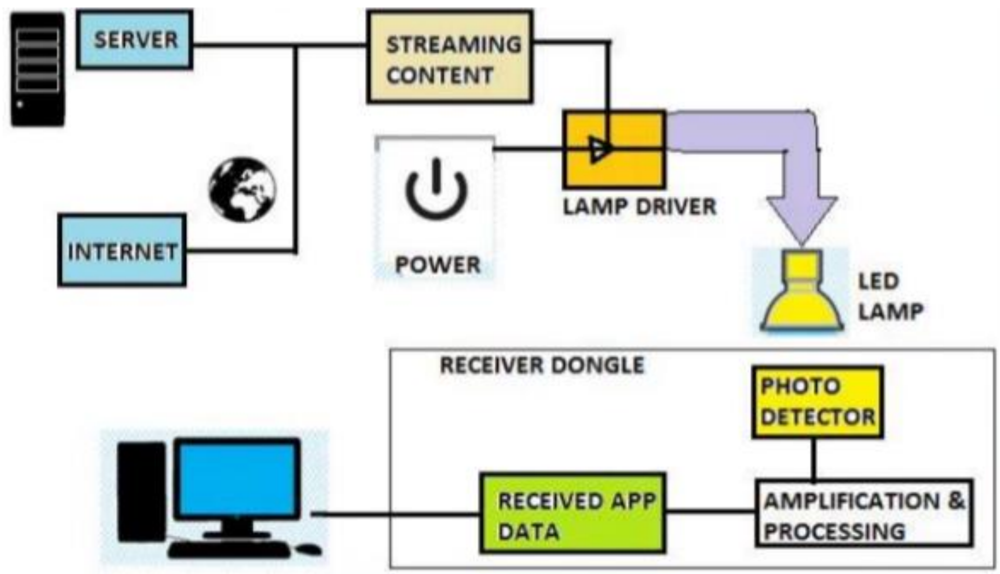

Figure 2.5 Working principles of general VLC system

A server is a system (software or suitable computer hardware) that responds to request across a computer network to provide a network service. Internet and server run in parallel. When we type a site for example –google.com, it sends request to various servers and finally sending request to the servers of Google in USA. Finally, after analyzing the request Google server sends as the required information in various packets .All this happens in a few seconds. From the figure the lamp driver contains the following components of light driver. These are baseband modulator, digital-to-analog converter (DAC), transistor arc control (TAC) and adder.

CHAPTER THREE

3. SYSTEM MODEL

The system model considered in this thesis consists of a VLC AP and K multiple users, where K is the number of triples. The users are classified into three sets, set Us of K users, defined as strong users, which are the users with strong VLC channels, set U_i of K users, which are the users with intermediate VLC channel gain users and set Uw of K weak users, which are the users with the weak VLC channels. In this research, a VLC cell with single LED (transmitter) serving K users (photo detectors or receivers) can be considered. In VLC system, there are two types of channels as RF did. These are line of sight (LOS) and non-line of sight (NLOS) downlink channel model is observed. It can be also assumed that a perfect SIC at the receiver.

3.1. Line of sight (LOS) VLC indoor channel model

In [18],derives the first and simplest case that one should consider is LOS (line of sight) channel, without the reflecting contribute, with a point Lambertian light source and continual received irradiance. This can be achieved by imposing the condition that the transmitter receiver square distance (d) is larger than receiver surface ($(A_r) : d^2 >> A_r$.

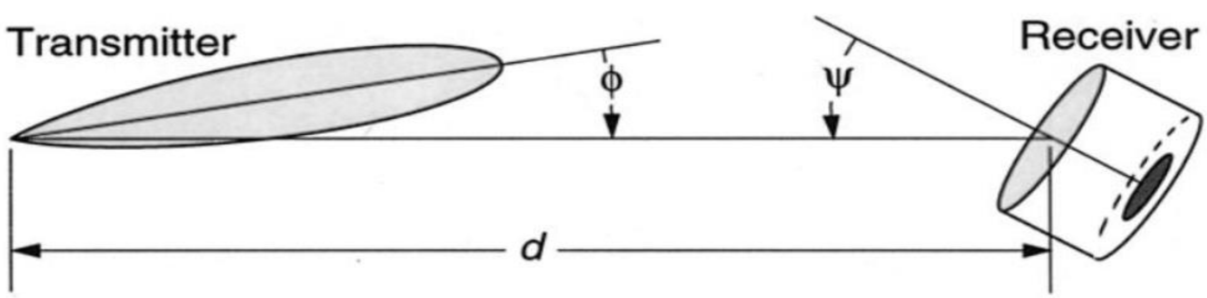

Figure 3.1 Transmitters to receiver LOS path from [12]

The approximation used before brings to constancy of the luminous flux on:

$$d^2 >> A_r \rightarrow \int_{A_r} P_r * \hat{n} dA_r = P_r * A_r \text{..} 3.1$$

Where Pr is received power

This equation describes the constancy of the luminous flux implies simplification of the area integral. The angular distribution of the optical radiation might be well-defined by Lambertian radiant intensity:

$$R_0(\phi) = \begin{cases} \frac{(m_l + 1)}{2\pi} \cos^{m_l}(\phi),\ for\phi \in \left[\frac{-\pi}{2}, \frac{\pi}{2}\right] \\ 0,\ for\phi \geq \frac{\pi}{2} \end{cases} \quad \text{...3.2}$$

Where m_l is the Lambert's mode number a way to describe the directionality and ϕ is the angle between the LED normal and d (vector that connect transmitter and receiver).

The Lambertian mode is related to LED semi angle; this parameter can be found on the LED datasheet:

$$m_l = \frac{-\ln 2}{\ln(\cos\phi_{\frac{1}{2}})} \quad \text{...3.3}$$

This equation calculates the order of Lambertian emission.

The effective area of receiver photodiode is centered on the receiver surface inclination. One must project the surface on the axis d that links transmitter and receiver.

$$A_{eff}(\psi) = \begin{cases} A_r \cos(\psi), 0 \leq \psi \leq \frac{\pi}{2} \\ 0, \psi > \frac{\pi}{2} \end{cases} \quad \text{...3.4}$$

This equetion expreses the receiver surface projection,where A_r is the area of the receiver photodiode, ψ is the angle between the photodiode normal and d.

To evaluate the LOS channel one should multiply all the factors found until now to obtain:

$$H_{LOS}(0) = A_r \frac{(m_l + 1)}{2\pi d^2} \cos^{m_l}(\phi) T_S(\psi) \cos(\psi) \quad \text{...3.5}$$

Where $H_{LOS}(0)$ is DC LOS gain, m_l is the Lambert's mode number, ψ is the angle between the photodiode normal and d, ϕ is the angle between the LED normal and d. $T_S(\psi$ is the gain of optical filter, which permits the transmission of specific wavelength. In addition, the d square expresses the relation in equation equ.3.1. This is the channel gain, now one can just multiply the line of sight (LOS) channel gain by the input optical power to obtain the power on the receiver:

$$P_r = H_{LOS}(0) P_t \quad \text{...3.6}$$

Where P_r is the received power, $H_{LOS}(0)$ is the DC channel gain, P_t is the transmitted power.

To define the impulsive optical gain it is essential multiply DC LOS gain with a Dirac's delta:

$$h_{los}(t) = A_r \frac{(m_l + 1)}{2\pi d^2} \cos^{m_l}(\phi) T_S(\psi) \cos(\psi) \delta\left(t - \frac{d}{c}\right) \quad \text{......................................3.7}$$

This equation expresses the impulsive optical power gain and it is derived from numerical algorithm.

3.2. Non line of sight indoor model

In indoor VLC systems, the LOS path is not the only path signal through which arrives at the receiver: there is alternative path that is produced from the light rays that bounce on the wall and furniture of the room. A more complex model can embrace NLOS to increase the arrival power or to overcome the absence of LOS channel. The NLOS channel is more complicated to model. In particular, it requires significantly more computing resources. The first attention which, has to be done for the NLOS channel regards the arrival time of the impulse. The impulses do not arrive all at the same time because the beam path is not the same for all the rays. The received power on the photodiode can then be expressed with the sum of the LOS and NLOS channel gain multiplied with the power transmitted[19]:

$$P_r = (H_{LOS}(0) + H_{NLOS}(0))P_t = \left(H_{LOS}(0) + \sum_{refl} H_{refl}(0) \right) P_t \quad \text{..................................3.8}$$

This expression is the total power received from line of sight (LOS) and non-line of sight(NLOS) path. One of the most used algorithms to model the NLOS path of VLC (OWC) system is presented in [20]. The condition of use of this algorithm encompasses a closed void room with Lambertian reflective walls. For an estimate, this situation is not so constrictive. Now the key is to consider the light as a summation of different endless rays that bounce through the room, the totality of these rays is the LOS plus the NLOS gain path. One ray is generated from the source element and hits a receiver element, the source and receiver element can be not only a LED and a photo receiver, but also the wall. For example if one takings one ray which is reflected from the wall,: in a first time the wall is well-thought-out as receiver and in a second time the wall receiver component can be considered as a transmitter with power proportional to received power multiply the wall reflection coefficient. This can be applied at each ray for each reflection. To represent one ray, one needs the path, that this ray runs from the LED to the photo receiver, after that the path can be viewed as a sum of "sub-rays" (for instance, From LED to wall ray plus from wall to photodiode ray), every of these rays can be symbolized with a source, a receiver, a path and a pulse. Therefore the impulse response can be modeled as the totality of all the sub-rays above mentioned[21]:

$$h(t,S,R_x)=\sum_{k=0}^{\infty}h^k(t,S,R_x)\text{...}3.9$$

This equation expresses one ray path with infinite multiple bounces, k is the bounce numbers, t is the time, and S is the source point.

3.3. General expression of indoor VLC modulations

The IM-DD technique is the utmost used method to converse with VLC for its small cost and for its easiness. Typical VLC use LEDs to communicate with photodiodes: the modulating signal is the current signal $m(t)$ that passes through the LED that generates the optical power output $x(t)$. In modest words, the modulation is based on the light power created from LED. The receiver is a photo detector that produces a photocurrent $y(t)$. The photocurrent (square law detector) is directly proportional to the optical power that impinges the photo detection surface.

3.4. VLC System Modeling

First, the parameters are booked and now we want to model the system. We are defining the mathematical equations, which, are used to scheme the method. The first parameter we want to think through is the lighting inside a room. To determine this parameter we want to calculate the luminous intensity, which determines the brightness of an LED. Luminous intensity is the luminous flux per solid angle and is given as[22]:

$$I_l=\frac{d\phi}{d\Omega}\text{...}3.10$$

Wherever Φ is the luminous flux and Ω is the spatial angle. Now we must to calculate the optical power *P* transmitted by all the LED arrays. It is used to calculate the radiation intensity generated by these LEDs. The transmitted optical power is given as[22]:

$$P=K\int_{A_{\min}}^{A_{\max}}\int_{0}^{2\pi}\phi_e\,d\theta d\lambda\text{...}3.11$$

In here, P is the total optical power generated, K is the maximum visibility (or) safety measures required for eyes, which are taken as 683lm/W, and the bandwidth is limited from LED to LED. For our consideration, we take it as 555 nm wavelength. Where $A_{\min}$ and $A_{\max}$ are determined from the photo diode sensitivity curve. LED lighting is emitted in the form of a Lambertian pattern (assumed), is the order of the m_l *or m* Lambertian emission and its equation is[23]

$$m_l = -\frac{\ln 2}{\ln(\cos\phi_h)} \text{...}3.12$$

Φ_h is defined as a half power semi-angle of an LED. ln is determined as the natural logarithm its values changes from that of a logarithm values Centre luminous intensity which is given by[24]

$$I(0) = (m_l + 1)/2\pi d^2 \text{..}3.13$$

The radiation intensity at a desk surface is given by[22]:

$$I(\phi_i) = I(0).\cos^m(\phi) \text{..}3.14$$

Where ϕ_i is the angle of irradiance in terms of the axis normal to the transmitter surface, m is Lambertian pattern and $I(0)$ is the Centre luminous intensity .the parameter that are, discussed is the effective area of a receiver (photo detector) the optical signal falls on the detector at the angle ψ ,the effective collecting area of the detector is given by[24]:

$$A_{eff} = A\cos(\psi) \qquad 0 < \psi < 90^0 \text{......................................}3.15$$

Not at all signals are taken into attention if the angle is greater than 90.

3.4.1. Lambertian (diffuse ideal) emission law

The Lambertian emission law states that the luminous intensity radiated from an ideal diffusely source identified from a viewer is directly proportional to the cosine of the angle between the surface normal and the direction of the spectator. This means which the light does not have the chosen path of reflection[25].

3.5. **Geometric Channel Model of VLC**

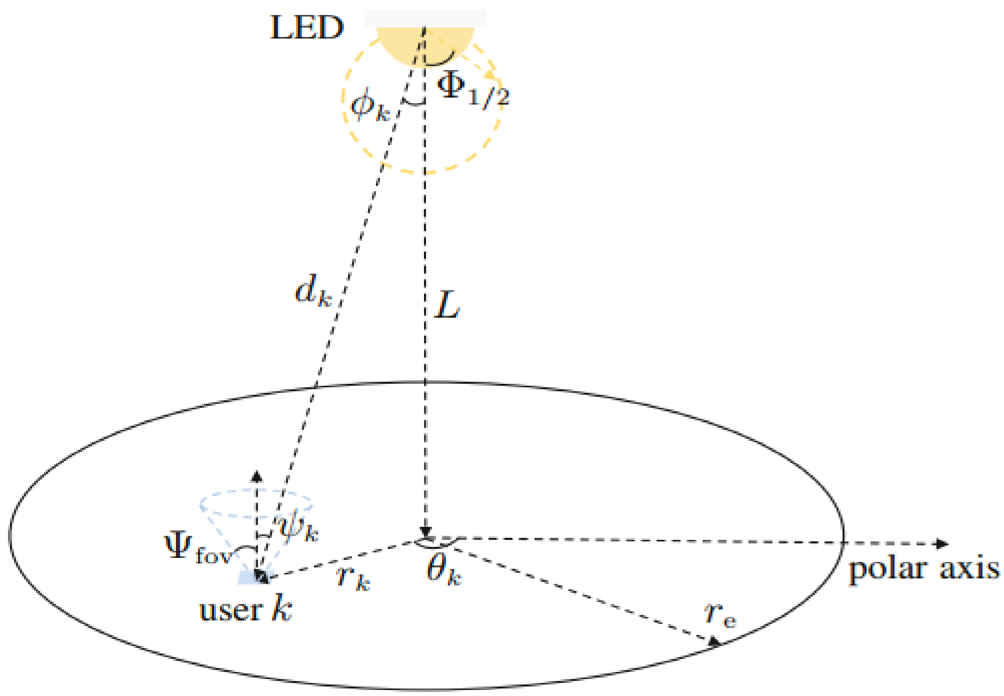

Figure 3.2 Downlink geometry of a VLC link

As shown in Fig3.2, this thesis consider a point-to-multipoint downlink transmission scenario, where an LED is located on the ceiling to simultaneously serve *K* random users that are uniformly distributed within a circular area. This geometrical model is an extension of the point-to-point VLC scheme to accommodate many users. In the following study, we assume which the users to be served are fixed or quasi-static hence that their channel gain is not outdated until the next channel estimation. A quasi-static process is a thermodynamic procedure that, occurs slowly adequate for the method to persist in internal equilibrium. The maximum cell radius is denoted by r_e, and L represents the vertical distance from the LED to the receiving plane. In a polar coordinate scheme, the position of an arbitrary user *k*, *k* = 1, 2… 12 Can be symbolized by (r_k, θ_k), where r_k represents its horizontal separation from the LED and θ_k represents its polar angle from the reference axis. Although the whole VLC channel comprises of not only the LOS link but also the NLOS constituents affected by light reflections from interior surfaces, earlier work has described which in a typical indoor environment the strongest diffuse component is at least 7 dB (electrical) lesser than the weakest LOS constituent [26]. For this motive, only the line of sight (LOS) link is considered in the theoretical study. The LED is assumed to follow a Lambertian radiation pattern whose order is given by[27]:

$$m = -\frac{1}{\log_2(\cos(\phi_{1/2}))} \qquad 3.16$$

Where $\phi_{1/2}$ denotes the semi-angle of the LED. The PD at each user assumed to be facing vertically upwards and its field of view (FOV) is denoted by ψ_{FOV}. In the line of sight (LOS) link, the Euclidean distance among the LED and user k is represented by d_k. The angle of irradiance and the angle of incidence are denoted by ϕ_k and ψ_k, respectively. Without loss of generality, we assume which all of the users are ordered based on their channel abilities:

$$h_1 \le h_2 \le \ldots \le h_k \le \ldots \le h_K \qquad 3.17$$

Where h_k represents the direct current channel gain of the line of sight (LOS) link among the LED and the k^{th} user, given by[28]:

$$h_k = \frac{(m+1)AR_{PD}}{2\pi d_k^2}\cos^m(\phi_k)\,g_f(\psi_k)\,g_c(\psi_k)\cos(\psi_k) \qquad 3.18$$

Where A symbolizes the detection area of the PD; R_{PD} represents the responsively of the PD; $g_f(\psi_k)$ represents the gain of the optical filter used at the receiver; and $g_c(\psi_k)$ represents the gain of the optical concentrator, given by [28]:

$$g_c(\psi_k) = \begin{cases} \dfrac{n_c^2}{\sin^2(\psi_{FOV})}, & 0 \le \psi_k \le \psi_{FOV} \\ 0, \psi_k > \psi_{FOV} \end{cases} \qquad 3.19$$

Where n_c is the reflective index of the optical concentrator used at the receiver front end, and it is defined as the ratio of the speed of light in free space and the phase speed of light in the optical material. For visible light, the typical values for n_c are between 1 and 2.

3.6. **Downlink OFDM-NOMA schemes in VLC**

In this thesis, a general *k*-user downlink NOMA system, where all users experience distinct channel gains can be considered. In *k*-user downlink NOMA, a particular transmitter (BS) non-orthogonally transfers *k* different signals over the similar VLC resources, where all *k* receivers

(UEs) receive their wanted signals alongside with the interferences produced by the communications of additional UEs. To obtain the desired signal, each SIC receiver first decodes the dominant interferences after that subtracts them from the superposed signal. Therefore, the established signal powers of the interference signals need to be adequately higher in contrast to the wanted signal in order to terminate them by SIC processing at the receiver end. Ever since each UE gets entirely signals (wanted and interfering signals) over the identical VLC spectrum (channel), multiplexing of different signals with different power levels is crucial to diversify each signal and to achieve SIC at a known UE receiver. In downlink NOMA, the messages of high channel gain customers are transferred with low power levels whereas the messages of low channel gain users are transmitted with high power levels. As such, at a specified receiver, the strong interfering signals are mostly due to the information of low channel gain customers. The weakest channel handler (who receives low interferences due to relatively low powers of the messages of high channel gain customers) cannot suppress any interference. Nevertheless, the maximum channel gain customer (who gets strong interferences owing to relatively high powers of the messages of small channel gain customers) can suppress altogether interfering signals[29].

3.6.1. Distribution function of the channel gain

By substituting, $d_k = \sqrt{r_k^2 + L^2}$, $\cos(\phi_k) = \frac{L}{\sqrt{r_k^2+L^2}}$ and $\cos(\psi_k) = \frac{L}{\sqrt{r_k^2 \ +L^2}}$ in to(3.18) ,the LOS channel gain can be expressed as

$$h_k = \frac{C(m+1)L^{m+1}}{(r_k^2 + L^2\,)\,\frac{m+3}{2}}\ , where\ C\ is\ given\ by{:}\ C = \frac{1}{2\pi} AR_{PD}\, g_f(\psi_k) g_c(\psi_k)$$

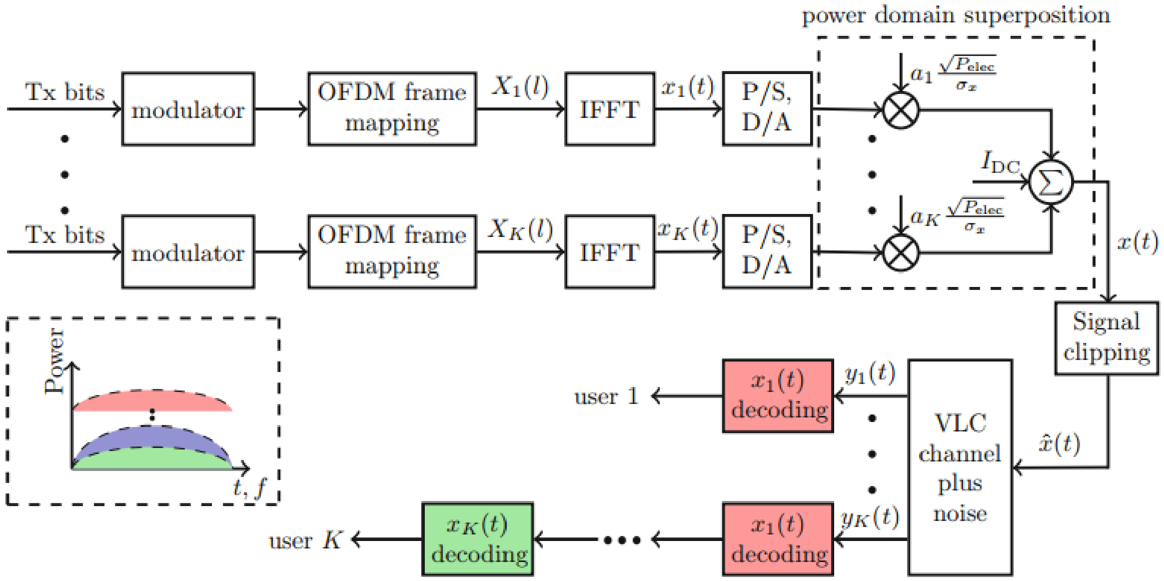

Figure 3.3 A general block diagram of NOMA principle for VLC[28]

In this thesis, the system discusses the use of DCO-OFDM in combination with NOMA for multiuser VLC[30]. A simplified block diagram illustrating the transmission/reception principle is shown in Fig3.3. First, K parallel information streams are produced, and every information stream is conducted to a modulator. According to the principle of OFDM, the information bits for each user are framed and mapped to complex symbols, $X_k(l)$ where $k = 1,2,..., K$, based on the selected modulation scheme. Here, l denotes the index of the subcarrier. Within every OFDM frame, the numeral of subcarriers, which carry information, is equal to $N_{FFT}/2-1$, where N_{FFT} the size of the inverse fast Fourier transform (IFFT) is and the size of the fast Fourier transform (FFT). This spectral efficiency (SE) damage is because of the Hermitian symmetry limitation:

$X_k(0) = X_k(N_{FFT}/2) = 0, X_k(l) = X_k^*(N_{FFT}-l)$ for $l = 1,2,..., N_{FFT/2}-1)$ .In order to make the time domain signal real, In general, a cyclic prefix (CP) is included in the OFDM subcarriers to combat inter-symbol interference (ISI). However, in VLC the CP is shown to have a negligible impact on the power and bandwidth efficiencies[31]. Therefore, CP is omitted here for simplicity. The time-domain signal that carries information for user k is denoted by $x_k(t)$, and it is obtained by performing the IFFT operation on $X_k(l)$:

$$x_k(t) = \frac{1}{\sqrt{N_{FFT}}} \sum_{l=0}^{N_{FFT}-1} X_k(l) \exp(\frac{j2\pi lt}{N_{FFT}}) \qquad 3.20$$

After parallel-to-serial (P/S) conversion and digital-to-analog (D/A) conversion, the time-domain signals for all K users are superposed in the power domain: Signal $x_k(t)$ is multiplied by factor $a_k \sqrt{p_{elec}} / \sigma_x$ and then summed up. With the addition of a positive DC bias I_{DC}, the overall combined signal, which consists of all the information for K users and the DC bias, can be written as[32]:

$$x(t) = \sum_{k=1}^{K} a_k \frac{\sqrt{P_{elec}}}{\sigma_x} x_k(t) + I_{DC} \qquad 3.21$$

Where P_{elec}, equal to the variance of $x(t)$, represents the total available electrical power of all the message signals, and a_k represents the power allocation coefficient for user *k*. Because of the overall power restraint, the power allocation coefficients essential to fulfill:

$$\sum_{i=1}^{K} a_i = 1 \qquad 3.22$$

According to the standard of NOMA, users with inferior channel conditions are allotted more signal power. This implies that $a_1 \geq ... \geq a_k \geq ... \geq a_K$.

3.6.2. Clipping Distortion of VLC

The nonlinear characteristic of typical LEDs[33] requires the transmitted optical signal to be clipped at both the bottom and top levels, yielding the clipped signal $\hat{x}(t)$. This double-sided signal cutting is expressed by the following transfer function[34]:

$$\hat{x}(t) = \begin{cases} I_{\min}, x(t) + I_{DC} \leq I_{\min} \\ x(t) + I_{DC}, I_{\min} < x(t) + I_{DC} < I_{\max} \\ I_{\max}, x + I_{DC} \geq I_{\max} \end{cases} \qquad 3.23$$

Where $I_{\min}$ and $I_{\max}$ are the minimum and maximum current levels for a typical LED to operate in the linear region, respectively. According to the Bussgang theorem, the clipped signal can be modeled as[31]:

$$\hat{x}(t) = \alpha(x(t) + I_{DC}) + Z_{clip} \qquad 3.24$$

Where $\alpha = Q(\rho_b) - Q(\rho_t)$ is an attenuation factor, with $Q(.)$ being the well-known Q-function; $\rho_t = (I_{\max} - I_{DC})/\sigma_x; \rho_b = (I_{\min} - I_{DC})/\sigma_x$ and Z_{clip} is the time-domain clipping noise. The cutting of a time-domain OFDM signal adjusts its mean and subsequently its average optical power. Because the unclipped signal is Gaussian distributed, the clipped signal follows a truncated Gaussian distribution, whose mean is given by:

$$\mathrm{E}[\hat{x}(t)] = \sigma_x \left(\rho_t Q(\rho_t) - \rho_b Q(\rho_b) - f_G(\rho_t) + f_G(\rho_b)\right) + I_{\min} \ldots\ldots\ldots\ldots\ldots\ldots 3.25$$

Where $f_G(\rho) = 1/\sqrt{2\pi}\exp(-\rho^2/2)$ is the probability density function (PDF) of the standard Gaussian distribution. After the received signal being passed through the FFT circuit, Z_{clip} is transformed into Gaussian noise with zero mean and variance $\sigma^2{}_{clip}$, given by[31]:

$$\sigma_{clip}^2 = \sigma_x^2 \begin{pmatrix} \alpha - \alpha^2 + \rho_b^2(1 - Q(\rho_b)) + \rho_t^2 Q(\rho_t) + \rho_b f_G(\rho_b) - \rho_t f_G(\rho_t) + \\ (f_G(\rho_b) - f_G(\rho_t) + \rho_b(1 - Q(\rho_b)) + \rho_t Q(\rho_t))^2 \end{pmatrix} \ldots\ldots 3.26$$

The alteration of the clipping noise on the info signal can be measured by the signal-to-clipping-noise ratio (SCR), well defined as:

$$SCR = \frac{\alpha^2 \sigma_x^2}{\sigma_{clip}^2} \ldots\ldots\ldots\ldots\ldots\ldots\ldots\ldots\ldots\ldots\ldots\ldots\ldots\ldots\ldots\ldots\ldots\ldots 3.27$$

It can be seen from (3.26) that smaller values of ρ_b and ρ_t give a lower clipping noise, that can be attained by reducing the variance of the transmit signal. To facilitate quantifying the effect of clipping noise, in this thesis the variables define as follows.

$$\xi = \min\left\{\frac{I_{DC} - I_{\min}}{\sigma_x}, \frac{I_{\max} - I_{DC}}{\sigma_x}\right\} \ldots\ldots\ldots\ldots\ldots\ldots\ldots\ldots\ldots\ldots\ldots\ldots\ldots 3.28$$

3.7. Receiver Noise of VLC

After propagating though the VLC channel, the transmitted VLC signal is subject to random noise processes before the PD at each receiver detects it. observe that inside the receiver circuit, the main noise sources are the thermal noise and shot noise, and together noise processes can be demonstrated as additive white Gaussian noise [35] with a total variance σ_{noise}^2, given by:

$$\sigma_{noise}^2 = \sigma_{shot}^2 + \sigma_{thermal}^2 \ldots\ldots\ldots\ldots\ldots\ldots\ldots\ldots\ldots\ldots\ldots\ldots\ldots\ldots\ldots\ldots\ldots 3.29$$

Where σ^2_{shot} and $\sigma^2_{thermal}$ are the variance of shot noise and thermal noise, respectively. Although the shot noise creates from both info signals and ambient light, the contribution of signal-induced shot noise is relatively lesser and hence can be omitted. The variance of the ambient induced shot noise is [35]:

$$\sigma^2_{shot} = 2q_e I_{bg} I_2 B \quad \text{............} 3.30$$

Where q_e is the elementary charge; I_{bg} is the background current; I_2 = 0.562 is the noise bandwidth factor; and B is the desired modulation bandwidth. The pre-amplifier circuits at the receiver, on the other hand, mainly cause the thermal noise. Among preamplifier designs, the Trans impedance type is generally used because of its large dynamic range and wide bandwidth. Here it can be assumed the use of a p-intrinsic-n (p-i-n) field-effect transistor (FET) as the Trans impedance amplifier. The variance of the thermal noise is given by[35]:

$$\sigma^2_{thermal} = \frac{8\pi k_B T_K}{G} C_{PD} A I_2 B^2 + \frac{16\pi^2 k_B T_K I_{FET}}{g_{FET}} C^2_{PD} A^2 I_3 B^3 \quad \text{............} 3.31$$

Wherever k_B is the Boltzmann continual; T_K is the absolute temperature; G is the open loop voltage gain; C_{PD} is the stationary capacitance of PD per unit area; I_{FET} is the FET channel-noise factor; g_{FET} is the trans conductance of the FET; and I_3 = 0.0868 is another noise-bandwidth factor.

From equ.3.30 and 3.31 we can get the electrical SNR expressed in terms of the photo detector responsivity R, received optical power and noise variance as

$$SNR = \frac{(RP_r)^2}{\sigma^2{}_{shot} + \sigma^2{}_{thermal}} \ldots\ldots\ldots 3.32$$

3.8. Non-Orthogonal Multiple Access (NOMA)

NOMA is an essential helping technology for the 5G wireless networks that come to the heterogeneous demands on lesser latency, extraordinary steadfastness, massive connectivity, better fairness, and extraordinary throughput. It is basically dissimilar than these multiple access systems that offer orthogonal access to the users either in time, frequency, code or space. In NOMA, every user functions in the same band and at the similar time where they are distinguished by their power levels[36][37].

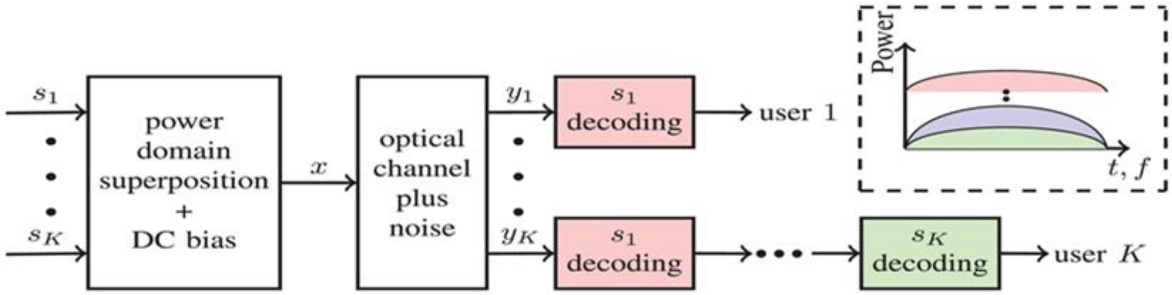

Figure 3.4 Block diagram of basic NOMA scheme with K users

In figure 3.4, the users are multiplexed in the power domain by assigning distinctive power levels to dissimilar users depending upon their channel conditions. The decoding method uses superposition coding (SC) at the transmitter side and successive interference cancellation at the receiver side. In this NOMA scheme all users can use the whole available bandwidth of the system which achieves superior spectral efficiencies[38].

3.8.1. Superposition Coding (SC)

The SC that was first suggested in [16] is a method of operating at the same time communicating info to dissimilar receivers by a distinct source. In other words, it permits the transmitter to transfer multiple users' information at the similar time. Instances of communications in a superposed fashion embrace broadcasting a television signal to multiple receivers and offering a speech to a group of people with different backgrounds and aptitudes, such as a lecture in a Classroom. Suppose a Doctor giving students information through a lecture in the classroom. Since there are dissimilarities among the abilities and backgrounds of the students, some of them obtain most of the information, and others obtain only a little. The lecture might be organized which it proceeds at the speed of the student with the weakest background. Nevertheless, in the ideal situation, the lecture can be planned in such a way which the students with the best suitable background obtain more information and the poor students catch at least the minimum amount of information. This situation is an instance of a broadcast channel where the speaker is delivering a superposed lecture. To make SC practical, the transmitter has to encode information relevant to each user. For instance, for a two-user scenario, the transmitter will must comprise two point-to-point encoders that draw their relevant inputs to complex-valued sequences of the two-user signal. Generally, SC is a multiuser transmission pattern, which intentionally presents interference amongst user signals at the transmitter, using a library of off-the-shelf point-to-point channel codes[39].

3.8.2.Successive Interference Cancellation (SIC)

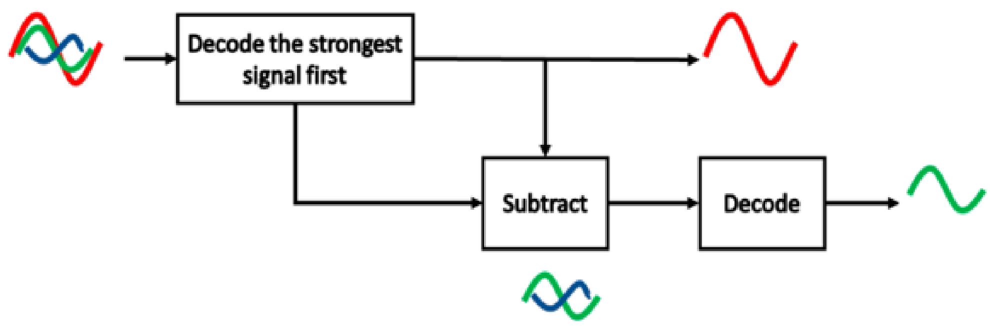

Figure 3.5 Successive interference cancelation (SIC) algorithms

To decode the superposed info at each receiver, cover first suggested the SIC method [16]. SIC is feasible by misusing terms on the dissimilarities in signal strength among the signals of need. The basic idea of SIC is which user signals are successively decoded. Afterward one user's signal is decoded, it is subtracted from the collective signal beforehand the next user's signal is decoded. When SIC is applied, one of the consumer signals is decoded, considering the other user signal as an interferer, however the latter is then decoded with the advantage of the signal of the previous having already been detached. Nevertheless, prior to SIC, users are well ordered according to their signal strengths, therefore that the receiver can decode the stronger signal first, subtract it from the collective signal, and separate the weaker one from the residue. Note that each user is decoded considering the other interfering users as noise in signal reception. In overall, SIC is a procedure that used through a receiver in a wireless data transmission , which licenses decoding of two or more packets, which reached simultaneously (in a fixed system, more packets reaching at the similar time cause a collision). SIC is attained through the receiver decoding the tougher signal first, subtracting it from the collective signal and then decoding the dissimilarity as the weaker signal. Generally, the procedures of successive interference cancelation is as follows[40]

1. The BS wants to recognize the perfect channel gain to organize the SIC decoding order that increases the CSI feedback overhead.

2. The SIC process familiarizes a higher computational complexity and delay at the receiver side, particularly for multicarrier and multiuser systems.
3. The strong users have to recognize the power allocation of the weaker users in order to perform SIC, which also raises the system signaling overhead.
4. Assigning high power towards the weak users, that are generally in the cell-edge, it tells more inter-cell interferences into the entire system

3.8.3. Decoding Complexity

Signal decoding by using SIC requires additional implementation complexity compared to orthogonal schemes, since the receiver has to decode other users' information prior to decoding its own information [41]. In addition, this complexity increases as the number of users in the cell of interest increases. However, users can be clustered into a number of groups, where each cluster contains a small number of users with bad channels.SC/SIC can then be executed within each group. This group wise SC and SIC operation provides a tradeoff between performance gain and implementation complexity[42].

3.9. Orthogonal frequency division multiplexing (OFDM)

OFDM is a very popular multiplexing method used for numerous of the modern wireless and telecommunication standards for example Wi-Fi 802.11ac, 4G cellular phone technologies, Wi MAX, satellite and lots of others. In OFDM, the channel is split in to a number of sub channels .The important property here is any two-sub channels are orthogonal to each other .Now each sub channel transmits a part of the original information .Every channel gives some bandwidth .So this available band width is divided in to N sub bandwidth, representing N sub-carriers.

The word "orthogonal" –means that two or multiple objects independently; in this case, any neighbor signals in OFDM operate without dependence on, or interference with one another. When the signal reaches its peak the highest point, its two neighbors are at their o point or at null. There for orthogonal means signals are multiplexed in a way that the peak of one signal occurs at null of the other neighbor signals[43].

3.10. User clustering

The proposed system exploits the channel gain differences amongst users and goals at enhancing the sum throughput of the well-thought-out cell. Prior to user grouping, this scheme relies on selecting a feasible number of clusters, i.e., decides on the number of clusters and in turn the number of users for each cluster. Once the number of users in a cluster is decided, user grouping is implemented. Let us consider an N-user downlink NOMA cluster to which ω units of resource blocks are allocated. The achievable throughput for UE_i, $\forall_i$ =1, 2… N, in an N-user downlink NOMA cluster can be expressed as[43]

$$\hat{R}_i = \omega B \log_2 (1 + \frac{P_i \gamma_i}{\sum_{j=N}^{i+1} P_j \gamma_i + \omega}), \forall_i = 1,2,..., N .... 3.33$$

Where $\gamma_i = \frac{h_i}{N_o B}$ is the normalized channel gain with N_o being the noise power spectral density, ω is the number of VLC channels assigned for the cluster, B is the transmission bandwidth of each channel i = 1; 2,… k, provides necessary insights to group users into a cluster. After SIC, the throughput of the maximum channel gain user in a cluster is not matter to the intra-cluster interference; instead, its throughput depends on its individual channel gain and power. Though the allotted transfer power for the highest channel gain user is small, its effect on the throughput is least. Consequently, if the gain of the highest channel is adequately high, then the attainable data rate negligibly depends on the transmission power; otherwise, the power is very low. Therefore, it is useful to dispense the high channel gain users in a cell into dissimilar NOMA clusters, as they can expressively give to the sum-throughput of a cluster. To raise the throughput of the customers with small channel gains, it is useful to pair them with higher channel gain users. The reason is that the higher channel gain users can achieve a higher rate even with low power levels while making a large fraction of power available for weak channel users. Here, the chief point of our task user clustering in downlink NOMA, is to make triple the highest channel gain user, the medium channel gain user and the lowest channel gain user into the same NOMA cluster, when the second highest channel gain user, the medium channel gain user and the second lowest channel gain user into another NOMA cluster, and so on. The throughput of the remaining users in a NOMA cluster follows the identical layout. That is, the manifestation for SINR comprises the similar channel in both the denominator and numerator, whereas the transmit power in the numerator is greater than the sum power in the denominator (this is specified by the SIC constraint). Here also we manipulate that, the throughput of the N users that mean N=1-12 in the NOMA cluster depends mostly on the spreading of the transmit power levels[44].

3.11. **Sum rate analysis**

In this research a single light emitting diode of downlink system with N users are considered. These N users are group in to clusters to maximize the sum rate of the system. The system uses a hybrid OFDM-NOMA approach, which means that the clusters are assigned the orthogonal resources so that there is no interference between them. However, users in the same cluster access the same resources. Thus, each cluster applies the NOMA technique and OFDM is applied among different clusters[45].

In NOMA systems, the signal-to-noise ratio (SNR) of the nth user is affected by the interference from the signals of users with higher channel gains, the signal to interference and noise ratio (SINR) for the nth user can be calculated by[46]:

$$SINR_n = \frac{a_n P_t (Rh_n \eta)^2}{P_t (Rh_n \eta)^2 \sum_{i=n+1}^{N} a_i + BN_o} \text{...} 3.34$$

Where B is the bandwidth and No is the noise power density. η is the photo diode efficiency are the responsibility photo diode.

The maximum sum rate in NOMA system is given by:

$$R_{sum}^{(NOMA)} = \sum_{n=1}^{N} B \log_2 \left(1 + \frac{a_n P_t (Rh_n \eta)^2}{P_t (Rh_n \eta)^2 \sum_{i=n+1}^{N} a_i + BN_o}\right) \text{....................................} 3.35$$

3.11.1. **NOMA Groups with 2 users**

For two users only the NOMA sum rate based on DCO-OFDM in the system can be expressed in the following relationship[47]. For $user_1$, having SINR = γ_1.

$$R_1 = \frac{1}{2} * B \log_2 (1 + \gamma_1) \quad \text{Here the unit is (bps)}$$

For $user_2$ having SINR = γ_2

$$R_2 = \frac{1}{2} * B \log_2 (1 + \gamma_2) \text{ (bps)}$$

$$R_T = R_1 + R_2 \text{..} 3.36$$

In the above equations, the coefficient indicates that half of the bandwidth is used for Hermitian symmetry[48].In Hermitian symmetry ,each expression is the sum of two exponentials; one containing a positive frequency and the other containing a negative frequency . In other words, when sine and cosine waves are written as complex numbers, the negative portion of the frequency spectrum is automatically included. The negative and positive frequencies are treated with an equal status; it requires one-half of each to form complete waveform.

3.11.2. **NOMA Groups with 6 users**

Now, let we have six users in the system .If we pair (2users) in single NOMA group we will have three NOMA groups.

NOMA $\text{group}_1 = (U_{11}, U_{12})$

NOMA $\text{group}_2 = (U_{21}, U_{22})$

NOMA $\text{group}_3 = (U_{31}, U_{32})$

Now rate for NOMA group_1 can be given as follows:

$$R_{11} = \frac{1}{2} * \frac{1}{3} * B \log_2(1+\gamma_{11})$$

$$R_{12} = \frac{1}{2} * \frac{1}{3} * B \log_2(1+\gamma_{12})$$

$$R_{1T} = R_{11} + R_{12}$$

Here, the half number is due to Hermitian symmetry and the number one-third (1/3) is due to the bandwidth is divided in to three NOMA groups. Similarly, we can do rate for NOMA group_2 and NOMA group_3 respectively.

$$R_{21} = \frac{1}{2} * \frac{1}{3} * B \log_2(1+\gamma_{21})$$

$$R_{22} = \frac{1}{2} * \frac{1}{3} * B \log_2(1+\gamma_{22})$$

$$R_{2T} = R_{21} + R_{22}, and$$

$$R_{31} = \frac{1}{2} * \frac{1}{3} B \log_2(1+\gamma_{31})$$

$$R_{32} = \frac{1}{2} * \frac{1}{3} B \log_2(1+\gamma_{32})$$

$$R_{3T} = R_{31} + R_{32}$$

Finally, the total sum rate of NOMA groups becomes:

$$R_T = R_{1T} + R_{2T} + R_{3T} \ldots\ldots\ldots\ldots\ldots\ldots\ldots\ldots\ldots\ldots\ldots\ldots\ldots\ldots\ldots\ldots\ldots\ldots\ldots\ldots.3.37$$

Now let us put three users in the NOMA group so for six users we will have two NOMA groups:

NOMA group$_1$= (U_{11}, U_{12}, U_{13})

NOMA group$_{2=}$ (U_{21}, U_{22}, U_{23})

The rate for NOMA group1 and NOMA group2 can be given as follows respectively.

$$R_{11} = \frac{1}{2} * \frac{1}{2} * B\log_2(1+\gamma_{11})$$

$$R_{12} = \frac{1}{2} * \frac{1}{2} * B\log_2(1+\gamma_{12})$$

$$R_{13} = \frac{1}{2} * \frac{1}{2} * B\log_2(1+\gamma_{13})$$

$$R_{1T} = R_{11} + R_{12} + R_{13}, and$$

$$R_{21} = \frac{1}{2} * \frac{1}{2} * B\log_2(1+\gamma_{21})$$

$$R_{22} = \frac{1}{2} * \frac{1}{2} * B\log_2(1+\gamma_{22})$$

$$R_{23} = \frac{1}{2} * \frac{1}{2} * B\log_2(1+\gamma_{23})$$

$$R_{2T} = R_{21} + R_{22} + R_{23}$$

Then the total sum rate of the two NOMA groups of six users in b/s/Hz can be written as follows.

$$R_T = R_{1T} + R_{2T} \ldots\ldots\ldots\ldots\ldots\ldots\ldots\ldots\ldots\ldots\ldots\ldots\ldots\ldots\ldots\ldots\ldots\ldots\ldots\ldots\ldots\ldots.3.38$$

3.11.3. **NOMA Groups with 12 users**

Now, let we have 12 users in the system (3 users) in a single NOMA group and (4 users) in a single NOMA group. Here we can get 4 NOMA groups with 3 users each and 3 NOMA groups with 4 users each respectively.

3.11.4. **Four NOMA Groups with three users each**

NOMA Group-1= (U_{11}, U_{12}, U_{13})

NOMA Group-2= (U_{21}, U_{22}, U_{23})

NOMA Group-3= (U_{31}, U_{32}, U_{33})

NOMA Group-4= (U_{41}, U_{42}, U_{43})

For NOMA Group one

$R_{11}=\frac{1}{2}*\frac{1}{4}*Blog2\,(1+\gamma_{11})$ [b/s]

$R_{12}=\frac{1}{2}*\frac{1}{4}*Blog2(1+\gamma_{12})$ [b/s]

$R_{13}=\frac{1}{2}*\frac{1}{4}*Blog2(1+\gamma_{13})$ [b/s]

$R_{1T}=R_{11}+R_{12}+R_{13}$

For NOMA Group two

$$R_{21}=\frac{1}{2}*\frac{1}{4}*Blog2(1+\gamma_{21}) \qquad [bps]$$

$$R_{22}=\frac{1}{2}*\frac{1}{4}*Blog2(1+\gamma_{22}) \qquad [bps]$$

$$R_{23}=\frac{1}{2}*\frac{1}{4}*Blog2(1+\gamma_{23}) \qquad [bps]$$

$$R_{2T}=R_{21}+R_{22}+R_{23}$$

For NOMA Group three

$$\mathrm{R}_{31}=\frac{1}{2}*\frac{1}{4}*\mathrm{Blog2}(1+\gamma_{31}) \qquad [\mathrm{bps}]$$

$$R_{32}=\frac{1}{2}*\frac{1}{4}*Blog2(1+\gamma_{32}) \qquad [bps]$$

$$R_{33}=\frac{1}{2}*\frac{1}{4}*Blog2(1+\gamma_{33}) \qquad [bps]$$

$$R_{3T}=R_{31}+R_{32}+R_{33}$$

For NOMA Group four

$$R_{41}=\frac{1}{2}*\frac{1}{4}*Blog2(1+\gamma_{41}) \qquad [bps]$$

$$R_{42}=\frac{1}{2}*\frac{1}{4}*Blog2(1+\gamma_{42}) \qquad [bps]$$

$$R_{43}=\frac{1}{2}*\frac{1}{4}*Blog2(1+\gamma_{43}) \qquad [bps]$$

$R_{4T} = R_{41} + R_{42} + R_{43}$

Finally the all total sum rate of NOMA groups with 12 users become as follows

$$R_T = R_{1T} + R_{2T} + R_{3T} + R_{4T} \dots\dots\dots\dots\dots\dots\dots\dots\dots\dots\dots\dots\dots\dots\dots\dots\dots\dots\dots\dots\dots .3.39$$

3.12. **User clustering methods**

In this thesis, users can be dividing as (high channel gain users, intermediate channel gain users, and low channel gain users) and it can be peak one users from subdivision to form the cluster. Here let us consider 12 total users with the following channel gain:

$h_1 \le h_2 \le \dots \le h_k \le \dots \le h_K$

If we decide to divide the users in to 3 subdivisions, we will have:

Subdivision A: $\{h_1, h_2, h_3, h_4\}$

Subdivision B: $\{h_5, h_6, h_7, h_8\}$

Subdivision C: $\{h_9, h_{10}, h_{11}, h_{12}\}$

Since two users from the same sub-division cannot be assigned for the same cluster (because their channel gain difference is small), the clusters become:

Cluster 1: $\{h_1, h_5, h_9\}$

Cluster 2: $\{h_2, h_6, h_{10}\}$

Cluster 3: $\{h_3, h_7, h_{11}\}$

Cluster 4: $\{h_4, h_8, h_{12}\}$

Therefore, those users in the same cluster can utilize PD-NOMA to share the same time-frequency resources at the same instant. In addition to this, for fixed number of users, when the number of users in a single cluster increases, the number of clusters in the system will decrease. Therefore, the objective is evaluating the performance of the system (based on sum-rate and BER) for fixed number of users by varying the power allocation coefficient based on channel gain for users in a cluster and without making the cluster in the system.

3.13. **Exact bit error rate (BER) expression of NOMA**

Bit error rate (BER) is an essential conception to understand in any digital transmission system since it is a main indicator of the health of the system. As data is transferred some of the bits may not be received appropriately .The more bits which are incorrect, the more the signal will be affected. It is important to know what portion of the bits is in error so we can determine how much margin the system has before failure. The performance of digital receiver is measured by a parameter called the bit error rate (BER).Bit error rate (BER) is expressed as the ratio of the number of incorrect bits over the number of all bits. That is, BER=number of bits in error/total bits transmitted or wrong bits per second/data rate in bits per second. The derivation of BER is as follows[49][50]:

$$BER = \int_0^\infty Q(\sqrt{a^2 SNR}) 2ae^{-a^2} da$$

Let the SNR= μ

BER= $\int_0^\infty Q(\sqrt{a^2 \mu}) 2ae^{-a^2} da$ but the Q function can be given by the following formula.

$$Q\,(v) = \int_v^\infty \frac{1}{\sqrt{2\pi}} e^{\frac{-t^2}{2}} dt$$

$$BER = \int_0^\infty \int_{\sqrt{a^2\mu}}^\infty \frac{1}{\sqrt{2\pi}} e^{-t^2/2} dt.2ae^{-a^2} da$$

Here, the inner integral is with respect to‘t’ and the outer integral is with respect to ‘a’.

Using substitution method,

$$\frac{t}{a\sqrt{\mu}} = u \;\; , dt = a\sqrt{\mu} du$$

$$BER = \int_0^\infty \int_1^\infty \frac{1}{\sqrt{2\pi}} e^{-\frac{u^2 a^2 \mu}{2}} * a\sqrt{\mu} du * 2ae^{-a^2} da$$

$$BER = \sqrt{\mu} \int_0^\infty \int_1^\infty \frac{2a^2}{\sqrt{2\pi}} e^{-\frac{a^2}{2}(2+\mu u^2)} duda$$

$$= \sqrt{\mu} \int_1^\infty \int_0^\infty \frac{2a^2}{\sqrt{2\pi}} e^{-\frac{a^2}{2}(2+\mu u^2)} dadu$$

In this derivation, the inner integral is with respect to ‘a’ and the outer integral is with respect to ‘ μ ’ by inter changing it.

$$\int_0^{\infty} \frac{2a^2 e^{-\frac{a}{2}^{2}}}{\sqrt{2\pi}} \left(2+\mu u^2\right) da = \delta^3$$

$$\delta^3 = \left(\frac{1}{2+\mu u^2}\right)^{\frac{3}{2}}$$

For a Gaussian distribution,

$$\int_{-\infty}^{\infty} \frac{t^2}{\sqrt{2\pi\delta^2}} e^{-t^2/2\delta^2} dt = \delta^2$$

$$\delta^2 = \frac{1}{2+\mu u^2} \Rightarrow \frac{1}{\delta^2} = 2+\mu u^2$$

$$2\int_0^{\infty} \frac{t^2}{\sqrt{2\pi}\delta} e^{-\frac{t^2}{2\delta^2}} dt = \delta^2$$

$$\int_0^{\infty} \frac{2t^2}{\sqrt{2\pi}} e^{-\frac{t^2}{2\delta^2}} dt = \delta^3$$

From the above equation of the inner integral with respect to a;

$$= \left(\frac{1}{2+\mu u^2}\right)^{\frac{3}{2}}$$

$$BER = \sqrt{\mu}\int_1^{\infty} \left(\frac{1}{2+\mu u^2}\right)^{\frac{3}{2}} du \,, u = \sqrt{\frac{2}{\mu}} \tan\theta \text{ and } du = \sqrt{\frac{2}{\mu}} \sec^2\theta d\theta$$

$$u = 1$$

$$\theta = \tan^{-1}\sqrt{\frac{\mu}{2}}$$

$$u = \infty$$

$$\theta = \tan^{-1}\infty = \frac{\pi}{2}$$

$$BER = \int_{\tan^{-1}(\sqrt{\frac{\mu}{2}})}^{\pi/2} \left(\frac{1}{2+2\tan^2\theta}\right)^{3/2} \sqrt{\frac{2}{\mu}} \sec^2\theta d\theta = \int_{\tan^{-1}(\sqrt{\frac{\mu}{2}})}^{\pi/2} \frac{\sqrt{2}}{2^{\frac{3}{2}}} \frac{1}{\sec^3\theta} \sec^2\theta d\theta = \frac{1}{2}\int_{\tan^{-1}(\sqrt{\frac{\mu}{2}})}^{\pi/2} \cos\theta d\theta$$

$$BER = \frac{1}{2}\sin\theta \,/_{\tan^{-1}\sqrt{\frac{\mu}{2}}}^{\frac{\pi}{2}}$$

$$= \frac{1}{2}\left(1 - \sin\tan^{-1}\sqrt{\frac{\mu}{2}}\right), but\ \sin\theta = \sqrt{\frac{\tan^2\theta}{1+\tan^2\theta}}$$

$$\sin(\tan^{-1}\sqrt{\frac{\mu}{2}}) = \sqrt{\frac{\tan^2\tan^{-1}\sqrt{\frac{\mu}{2}}}{1+\tan^2\tan^{-1}\sqrt{\frac{\mu}{2}}}} = \sqrt{\frac{\mu/2}{1+\mu/2}} = \sqrt{\frac{\mu}{2+\mu}}$$

Therefore, the average bit error rate (BER) formula of non-orthogonal multiple accesses in BPSK Rayleigh fading is as follows;

$$BER = \frac{1}{2}\left(1 - \sqrt{\frac{SNR}{2+SNR}}\right) \ldots\ldots\ldots\ldots\ldots\ldots\ldots\ldots\ldots\ldots\ldots\ldots\ldots\ldots 3.40$$

CHAPTER FOUR

4. RESULT AND DISCUSSION

As we have seen from thesis simulation result to achievable sum rates of power domain non-orthogonal multiple access (PD- NOMA) based on direct current optical orthogonal frequency division multiplexing (DCO-OFDM) in visible light communication channel system of simulation results N- number of users scenario. From this scenario by using a single user, two users, six users, and twelve users evaluate the performance of OFDM-NOMA in visible light communication. The following simulations are different parameters DCO-OFDM based NOMA-VLC system. Here a table has the parameters and specific value of the thesis.

Table 4 simulation parameters and its specific value[38][28][51]

No	Parameter name and notation	Parameter values
1	Separation between LED and PD, L	3m
2	Cell radius r_e	6m
3	Total number of users, K	12
4	LED semi-angle, $\phi_{1/2}$	60^o
5	Total signal power, P_{elec}	10watts
6	PD FOV, ψ_{fov}	60^o
7	PD responsivity, Rp	0.4A/w
8	PD detection area, A	$1cm^2$
9	Reflective index, n	1.5
10	Optical filter gain ,T	0.9
11	Signal band width B	20MHz
12	Noise PSD, No	$10^{-21} A^2 / Hz$
13	Modulation index	0.5
14	OFDM frame size, N_{FFT}	512

4.1. **Simulation results of two users in the system**

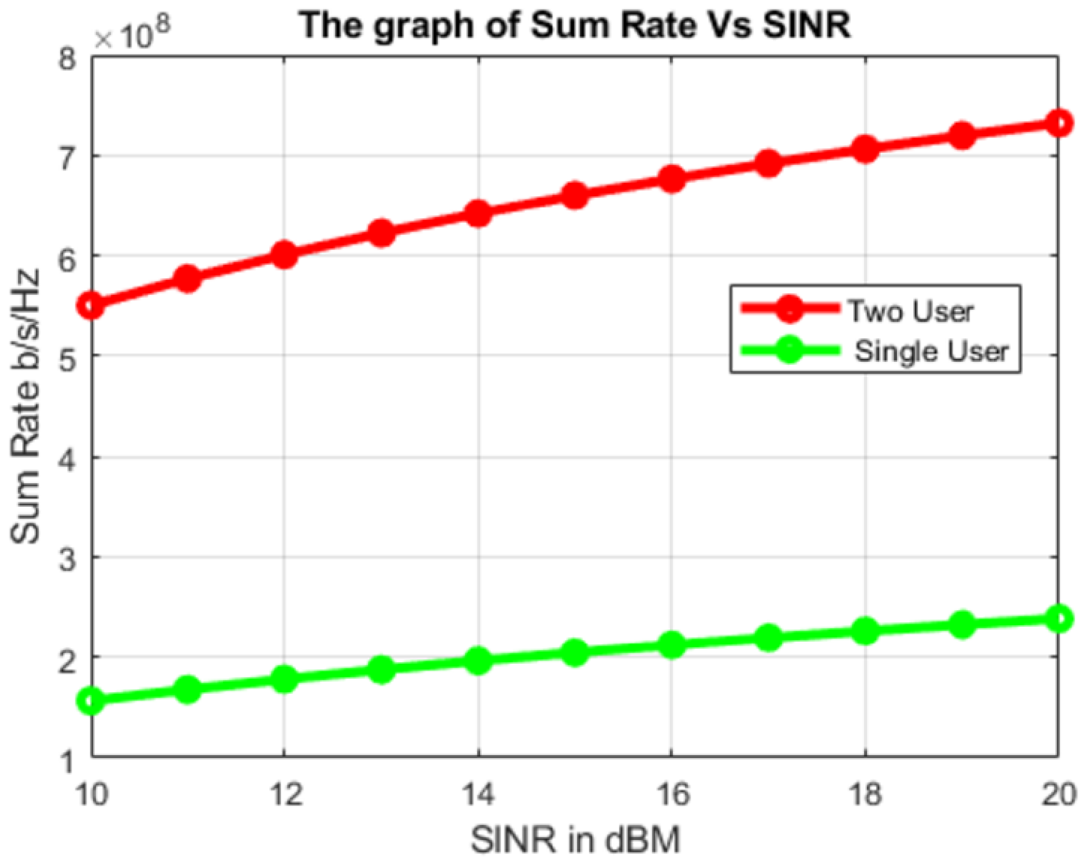

Figure 4.1 Sum rate versus SINR of two user and single user

As we have seen from the simulation result, figure 4.1 when we the symbol rate increase it also the SNR increase. The symbol rate was directly proportional to the signal to noise ratio. When we compare from the graph of single-user shows slowly change when SNR and symbol rate increase, because the effect can be observed in the sum of two or more users. In the above-simulated result figure 4.1, the signal to noise ratio increase the sum rate also increases. Since ,the bandwidth is a limited resource when the bandwidth decreases the efficiency of the system increase.

4.2. Simulation results of six users in the system

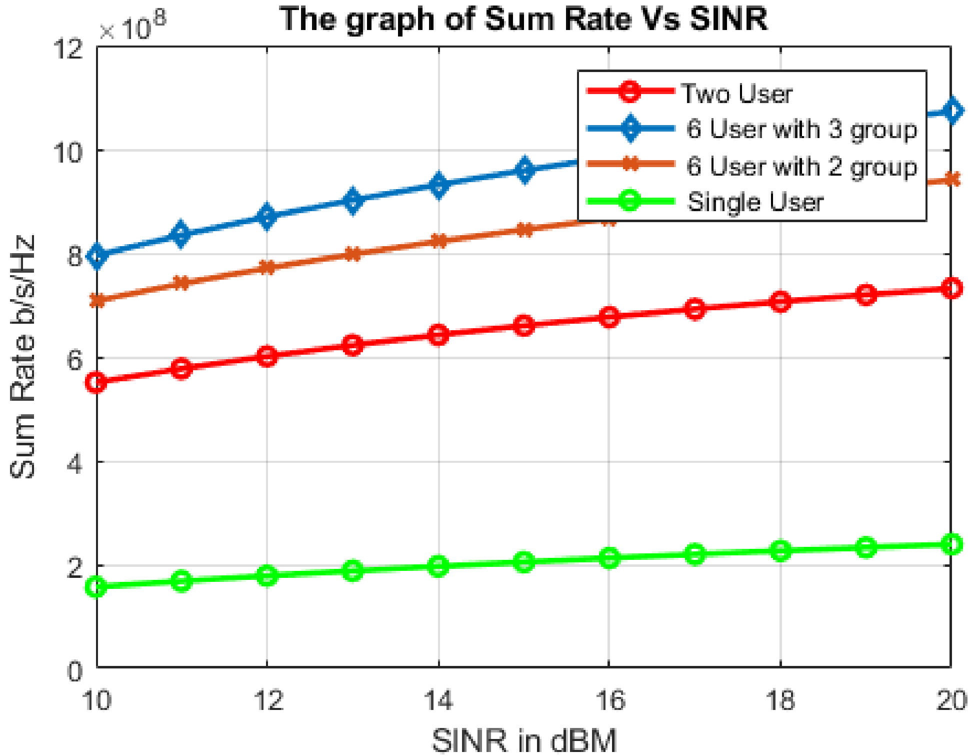

Figure 4.2 Sum rates versus SINR of six user, two user and single user

From this simulation figure 4.2, when the NOMA group increases the performance of the system increases and when the NOMA group decreases the sum rate decreases. Because when we observe the six users in the system, if we pair two users in single NOMA group we have three NOMA groups. Here half of the Hermitian symmetry and the number of groups divide the bandwidth. Moreover, we can put three users in single NOMA groups; so for six users we will have two NOMA groups. Here also half of the Hermitian symmetry and the number of groups divide the bandwidth. Generally from the simulation graph, when the number of NOMA groups increase the sum rate of the system increase. And also when the SINR increases the sum rate increase as we have observed from the simulation figure of 4.2.

4.3. Simulation results of twelve users in the system

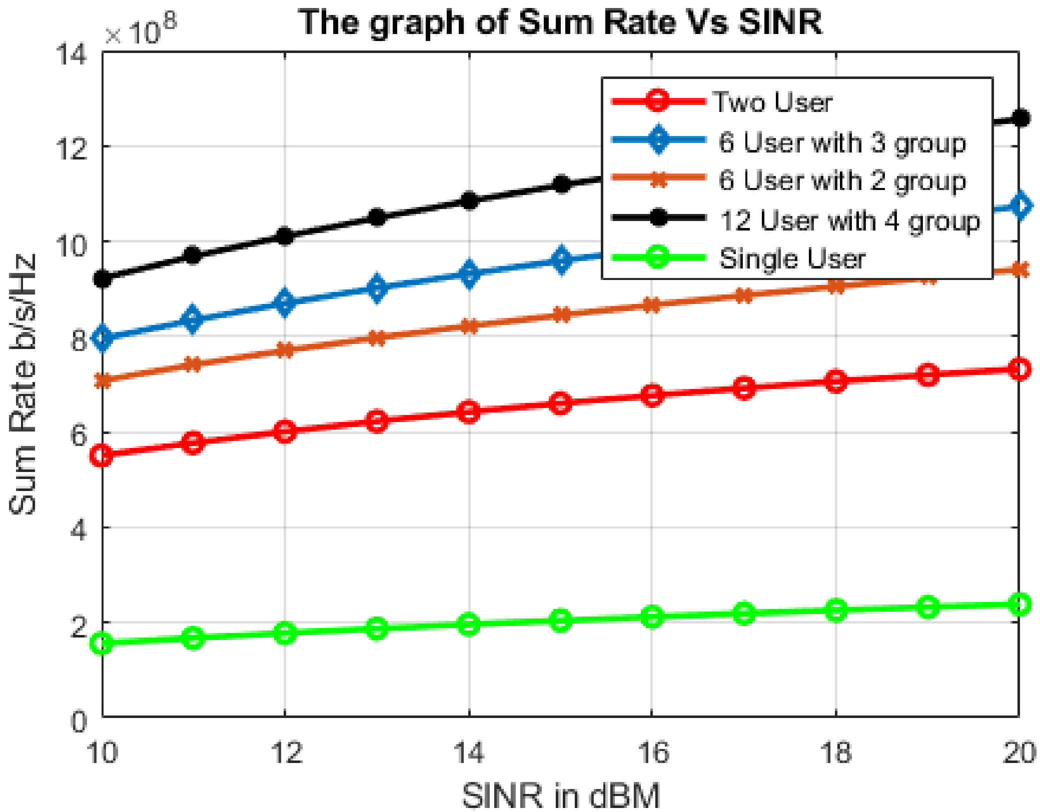

Figure 4.3 Sum rates versus SINR of twelve users, six user, two user and single user

From this graph having 12 users in the system and 3 users in a single NOMA group .Here we can get four NOMA groups with three users each and when the number of users increases the NOMA group increase. From this observation, as the NOMA group increase the sum rate increase and also, when the signal to noise ratio increase the performance of the system increase. Therefore, in this graph 12 users having 4 groups in each group 3 users have the best performance. Generally ,when the number of groups increase the sum rate increase as we have seen from the simulation result of black line in figure 4.3 and when the SINR increases the sum rate increase from this graph.

4.4. Clustering of 12 users based on channel gain difference

In this thesis, the simulation results are obtained for the designated OFDM-NOMA system in visible light communication (VLC) channel, which has the access point of light emitting diode (LED) communicating with twelve (12) users like that of photo diodes (PD) .In this simulation we assume that UE1, UE2, UE3, UE4 are far users and UE5, UE6, UE7, UE8 are medium users and UE9, UE10, UE11, UE12 are near users based on CSI of Euclidean distance.

4.4.1. Simulation results of cluster one

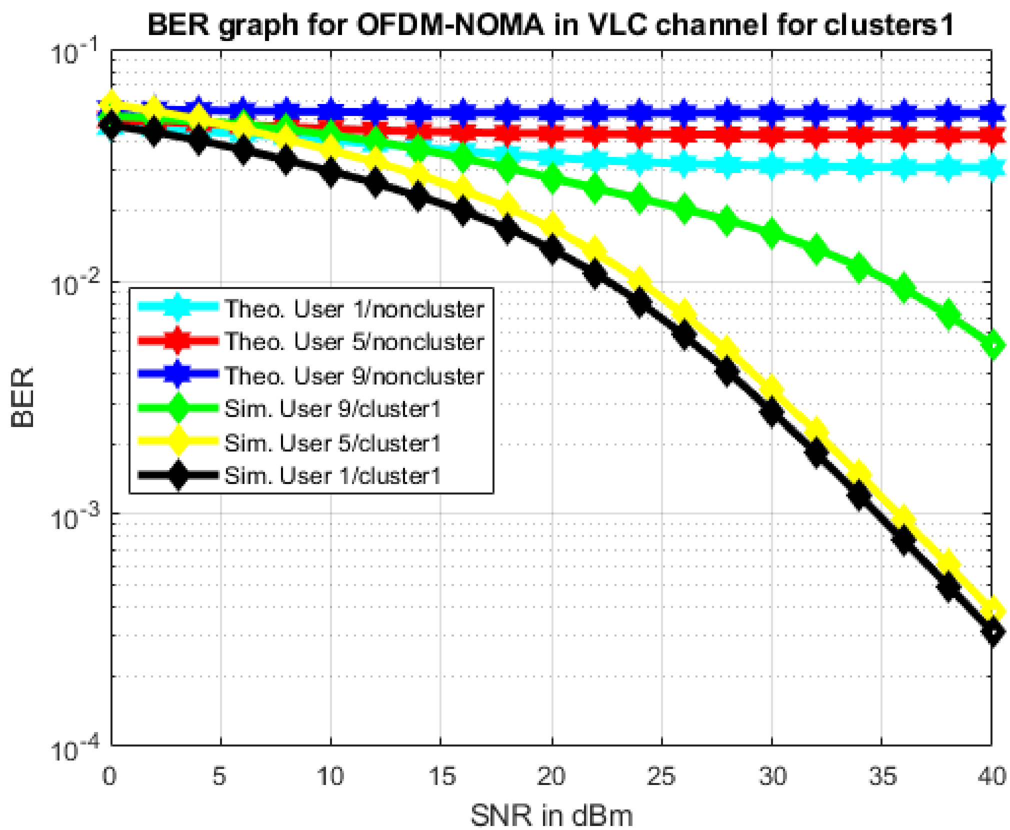

Figure 4.4 Simulation results of cluster 1

From the graph of simulation result in cluster 1 having $user_1$, $user_5$ and $uesr_9$, each user has the power allocation coefficients of a_1=0.2125, a_5=0.0925, a_9=0.04 and the distance between the access point and the user d1=6.71, d5=5, d9=3.61.based on this parameter, when the signal to noise ratio increases the bit error rate of each user in the cluster decreases and the non- cluster or the theory of OFDM-NOMA in VLC channel system also, a little bit decrease. we conclude that the clustered user has better bit error rate compared to non-clustered one or theory. In the theory of simulation we assume all users what we have taken for our thesis the channel gain difference is so small. They are near to each other in the visible light communication .Because of this, the interference among users created and so, the bit error (BER) is increased compared to the users, which make the cluster. The clustered users have less amount of bit error rate. This effect exists by their channel state information or channel gain difference becoming higher than non-clustered one that considers the power allocation coefficients arranging the users by the Euclidean distance. The same is true for cluster2, cluster3 and cluster4.

4.4.2. Simulation results of cluster two

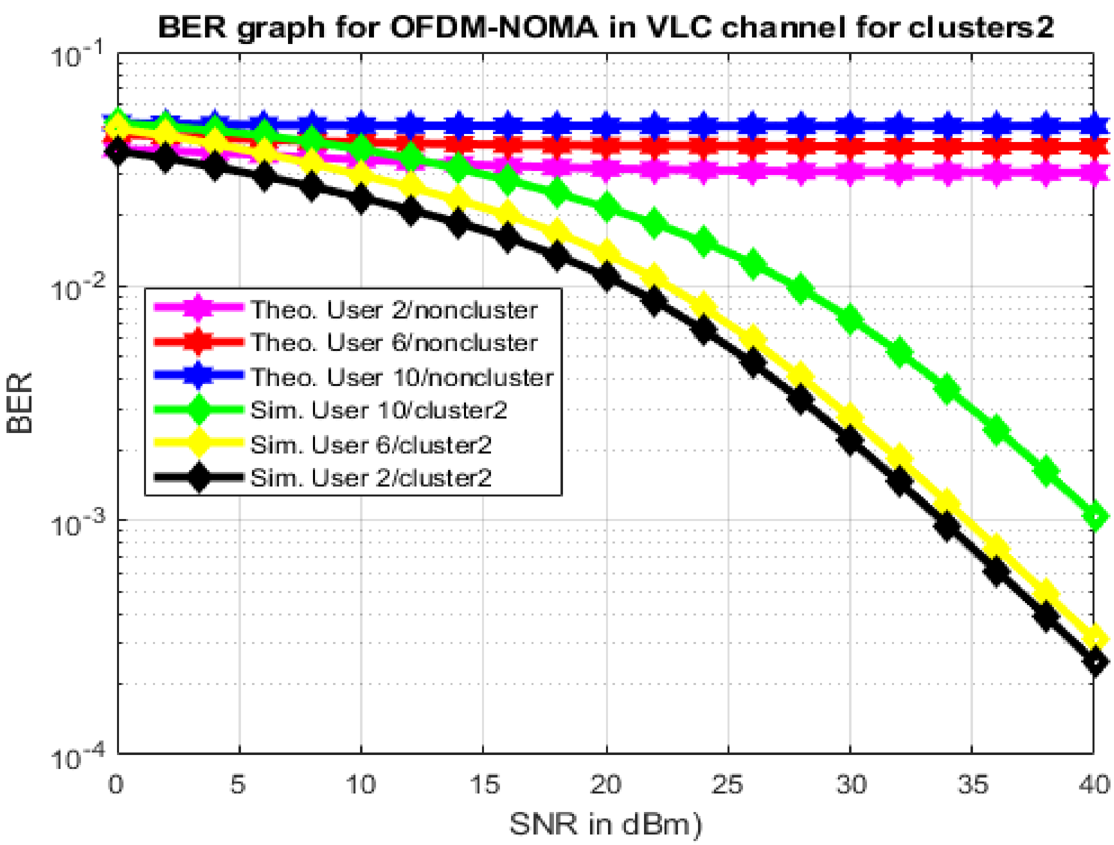

Figure 4.5 Simulation results of cluster 2

From the graph of simulation result in cluster 2 having $user_2$, $user_6$ and $uesr_{10}$ each user has the power allocation coefficients of a_2=0.1625, a_6=0.0825, a_{10}=0.03 and the distance between the access point and the user d2=6.27, d6=4.61, d10=3.35.based on this parameter, when the signal to noise ratio increases the bit error rate of each user in the cluster decreases and the non-cluster or the theory of OFDM-NOMA in VLC channel system also, a little bit decrease. We conclude that the clustered user has better bit error rate for each user compared to non-clustered one or theory. Because the cluster users have high channel state information than non-cluster one based on power allocation coefficients and Euclidean distance

4.4.3. Simulation results of cluster three

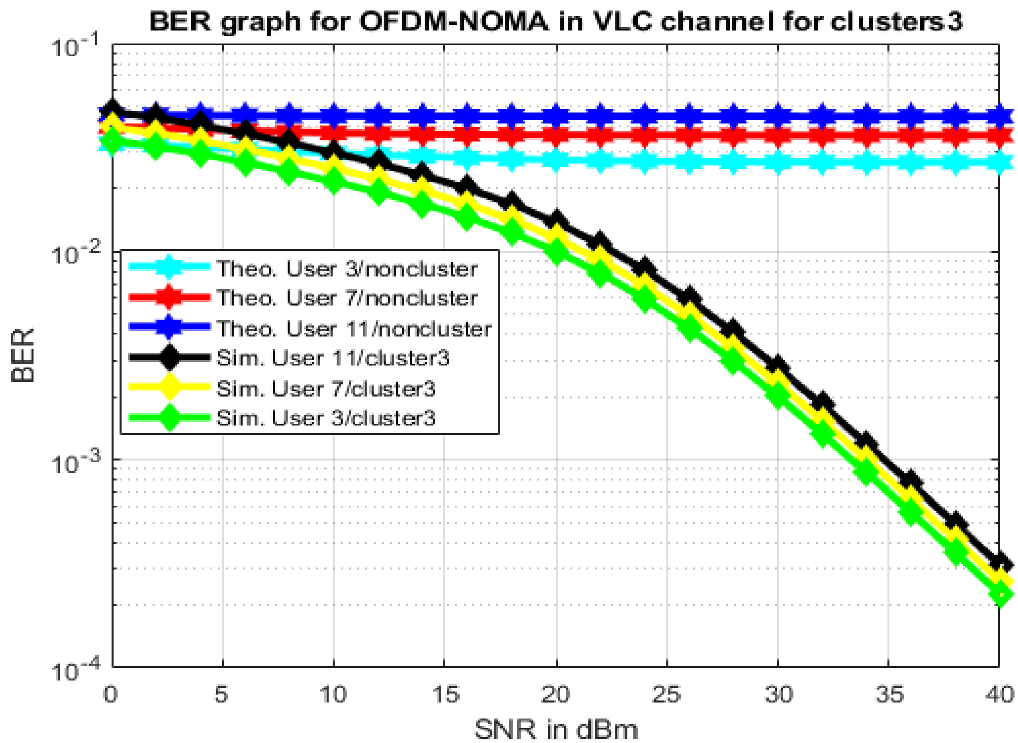

Figure 4.6 Simulation results for cluster 3

From the graph of simulation result in cluster 3 having $user_3$, $user_7$ and $uesr_{11}$ each user has the power allocation coefficients of a_3=0.1125, a_7=0.0725, a_{11}=0.02 and the distance between the access point and the user d3=5.83, d7=4.24, d11=3.16.based on this parameter, when the signal to noise ratio increases the bit error rate of each user in the cluster decreases and the non- cluster or the theory of OFDM-NOMA in VLC channel system also, decrease a few amount.

We conclude that the clustered user has better bit error rate for each user compared to non-clustered one or theory. Because the cluster users have high channel gain difference than the theory one based on the power allocation coefficient and Euclidean distance.

4.4.4. Simulation results of cluster four

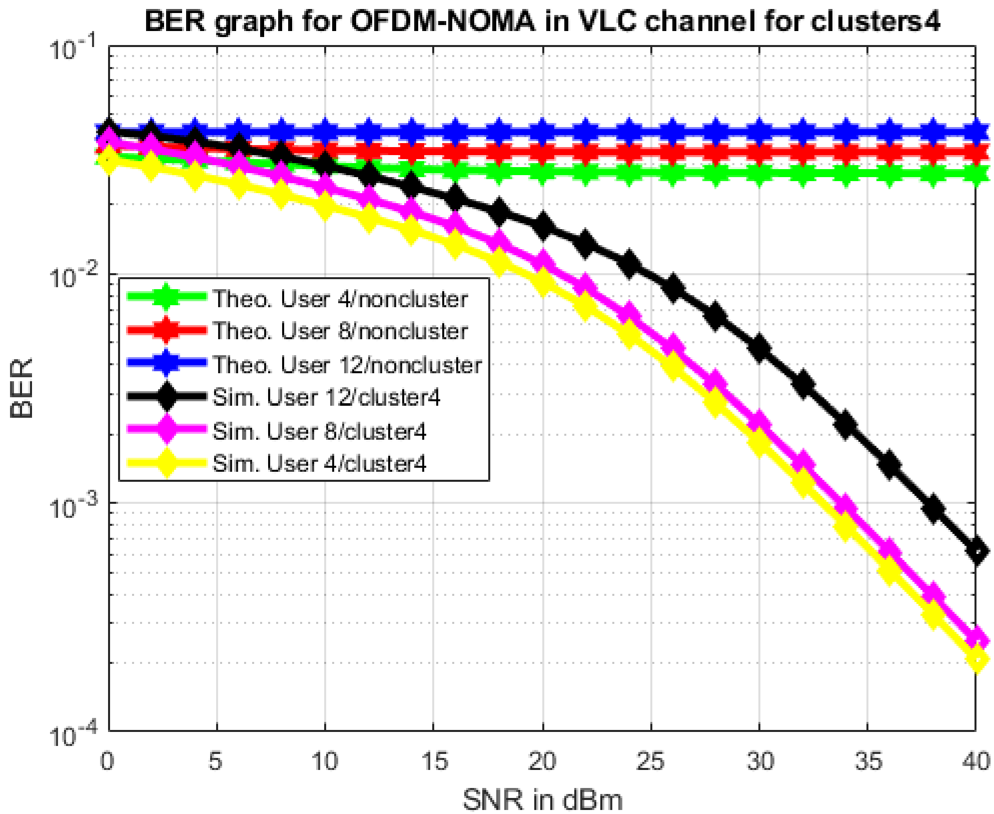

Figure 4.7 Simulation results of cluster 4

From the figure 4.7 of the simulation result in cluster 4 having $user_4$, $user_8$ and $uesr_{12}$ each user has the power allocation coefficients of a_4=0.1025, a_8=0.0625, a_{12}=0.01 and the distance between the access point and the user d4=5.41, d8=3.91, d12=3.04.based on this parameter, when the signal to noise ratio increases the bit error rate of each user in the cluster decreases and the non-cluster or the theory of OFDM-NOMA in VLC channel system also, a small amount decreases.

We conclude that the clustered user has better bit error rate for each user compared to non-clustered one or theory. Because the cluster users have high channel gain difference than non-cluster one based on the power allocation coefficient and Euclidean distance.

CHAPTER FIVE

5. CONCLUSIONS AND RECOMMENDATION

5.1. CLUSIONSCON

In this thesis, the performance of OFDM-NOMA system in visible light communication (VLC) channel has been observed .the analysis is based on the study of bit error rate (BER) reduction by clustering multi-users and sum rate maximization with grouping the users in different grouping schemes. Also it has been explained the design and different terms of OFDM-NOMA system in visible light communication channel.

From the simulation results, the sum rate maximization with different groups by making variable the bandwidth in terms of Hermitian symmetry and number of groups and the bit error rate (BER) of multi-users making a cluster the users based on channel gain or channel state information (CSI) in an indoor visible light communication is an important figure of merits which used to quantify the integrity of data transmitted through the communication system. By implementing the four different clusters, which have three users in each type, the criterion is comparison of the variation in bit error rate for different channel gains of the transmitted power in each cluster. Here it is observed that the bit error rate (BER) is less in clustered users than non-clustered users or the theory in the visible light communication channel of OFDM-NOMA system. Here also the performance of sum rate maximization has been observed in the simulation by varying the number of groups and dividing the bandwidth. Because in bandwidth efficiency or spectral efficiency, if the system uses less number of the bandwidth the system is efficient and the sum rate increases since the bandwidth is scares resource in electronic communication and if the system uses more amount of bandwidth the system is not spectrally efficient .The reason what the efficient system of the capacity is given by the transmitted bit rate divided by the band width in every communication system. That is when the bandwidth in the given group, increase the sum rate decrease and vice versa.

Generally, as we conclude from the performance of multi-user OFDM-NOMA in visible light communication channel, the clustered user has a better bit error rate (BER) which means; having less amount of bit error rate than what the theory or non-cluster says. And also we conclude that, having less amount of bandwidth has a better performance than having more amount of band width. In addition to this, when the SNR increases the sum rate increases and vice versa.

5.2. RECOMMENDATION

Furthermore, this work can be extended to increase the performance by using dynamic power allocation coefficients rather than fixed power allocation coefficients. That is, we have fixed the value of power allocation coefficients of the channel conditions .But there are enhanced ways to optimize power allocation coefficients dynamically based on the value of channel state information (CSI).

In this thesis also we recommend a novel method to decode the multiple users' signals from the super imposed signal ,where high order M-QAM signals are used .This decoding method is called ergodicity and comparison (EAC) .It is different from SIC method ;the EAC can recover the signals for multiple users simultaneously ,instead of decoding them one by one.

REFERANCES

[1] Y. S. Ero, "Slow Beam Steering and NOMA for Indoor Multi-User Visible Light Communications," pp. 1–30.

[2] S. Tao, S. Member, H. Yu, Q. Li, and Y. Tang, "SPECIAL SECTION ON GREEN SIGNAL PROCESSING FOR Strategy-Based Gain Ratio Power Allocation in Non-Orthogonal Multiple Access for Indoor Visible Light Communication Networks," *IEEE Access*, vol. 7, pp. 15250–15261, 2019.

[3] H. Marshoud, S. Muhaidat, P. C. Sofotasios, S. Hussain, M. A. Imran, and B. S. Sharif, "Optical Non-Orthogonal Multiple Access for Visible Light Communication," pp. 1–6.

[4] E. M. Almohimmah, M. T. Alresheedi, A. F. Abas, and J. Elmirghani, "A Simple User Grouping and Pairing Scheme for Non-Orthogonal Multiple Access in VLC System," *2018 20th Int. Conf. Transparent Opt. Networks*, pp. 1–4, 2018.

[5] H. Asif, S. Baig, S. Mumtaz, and S. Alrubaye, "Optimization of Non-Orthogonal Multiple Access based Visible Light Communication Systems," no. January, 2019.

[6] S. Tao, Y. Zuo, Q. Li, and Y. Tang, "Power Allocation of Non-Orthogonal Multiple Access with Variable on-off Keying Dimming Control in Visible Light Communication Networks Power Allocation of Non-Orthogonal Multiple Access with Variable on-off Keying Dimming Control in Visible Light Communic," *2018 IEEE 18th Int. Conf. Commun. Technol.*, no. May 2019, pp. 321–325, 2018.

[7] J. Shi, Y. Hong, R. Deng, J. He, L. Chen, and G. Chang, "Real-time Demonstration of Software Reconfigurable Dynamic Power-and-subcarrier Allocation Scheme for OFDM-NOMA based Multi-user Visible Light Communications," *2019 Opt. Fiber Commun. Conf. Exhib.*, pp. 1–3, 2019.

[8] Y. Fu, S. Member, Y. Hong, and S. Member, "Enhanced Power Allocation for Sum Rate Maximization in OFDM-NOMA VLC Systems," *IEEE Photonics Technol. Lett.*, vol. 30, no. 13, pp. 1218–1221, 2018.

[9] H. Ren *et al.*, "Performance Improvement of M -QAM OFDM-NOMA Visible Light Communication Systems," *2018 IEEE Glob. Commun. Conf.*, pp. 1–6, 2018.

[10] S. M. R. Islam, N. Avazov, O. A. Dobre, and K. Kwak, "Power - Domain Non - Orthogonal Multiple Access (NOMA) in 5G Systems : Potentials and Challenges," no. c, pp. 1–42, 2016.

[11] A. Al-Kinani, C. X. Wang, L. Zhou, and W. Zhang, "Optical wireless communication channel measurements and models," *IEEE Commun. Surv. Tutorials*, vol. 20, no. 3, pp. 1939–1962, 2018.

[12] D. Gujjari, "Visible Light Communication," no. August, 2012.

[13] C. Di, L. Magistrale, I. N. Fisica, and T. Avanzate, "Università degli studi di torino," 2016.

[14] *Visible Light Communications*. .

[15] H. Abuella *et al.*, "Hybrid RF/VLC Systems: A Comprehensive Survey on Network Topologies, Performance Analyses, Applications, and Future Directions," *arXiv*, pp. 1–27, 2020.

[16] X. Chen, M. Wen, and S. Dang, "On the Performance of Cooperative OFDM-NOMA System with Index Modulation," *IEEE Wirel. Commun. Lett.*, vol. 9, no. 9, pp. 1346–1350, 2020.

[17] "Efficient OFDM Signaling Schemes For Visible Light Communication Systems."

[18] M. Irshad, W. Liu, M. N. Sohail, D. Qaiser, M. M. Uba, and M. M. Bilal, "An Indoor LOS & NON-LOS Propagation analysis using Visible Light Communication," vol. 7, no. 10, pp. 727–732, 2018.

[19] Z. Lu *et al.*, "Experimental demonstration of non-line-of-sight visible light communication with different reflecting materials using a GaN-based micro-LED and modified IEEE 802.11ac," *AIP Adv.*, vol. 8, no. 10, 2018.

[20] J. R. Barry, J. M. Kahn, W. J. Krause, E. A. Lee, and D. G. Messerschmitt, "Simulation of Multipath Impulse Response for Indoor Wireless Optical Channels," *IEEE J. Sel. Areas Commun.*, vol. 11, no. 3, pp. 367–379, 1993.

[21] T. Led, F. Response, T. White, L. E. D. Frequency, and R. Model, "Models of the Visible Light Channel," pp. 39–58.

[22] T. Komine, S. Member, and M. Nakagawa, "Fundamental Analysis for Visible-Light Communication System using LED Lights," vol. 50, no. 1, pp. 100–107, 2004.

[23] E. E. Tsiropoulou and P. Vamvakas, "Resource Allocation in Visible Light Communication Networks : NOMA vs OFDMA Transmission Techniques Resource Allocation in Visible Light Communication Networks : NOMA vs OFDMA Transmission Techniques," no. July, 2016.

[24] N. Nitish, "Implementation of Visible Light communications For Indoor Applications," no. September, 2018.

[25] E. M. Almohimmah and M. T. Alresheedi, "Error Analysis of NOMA-Based VLC Systems with Higher Order Modulation Schemes," *IEEE Access*, vol. 8, pp. 2792–2803, 2020.

[26] T. Fath and H. Haas, "Performance Comparison of MIMO Techniques for Optical Wireless Communications in Indoor Environments," vol. 61, no. 2, pp. 733–742, 2013.

[27] Z. Dong, T. Shang, Q. Li, and T. Tang, "Adaptive Power Allocation Scheme for Mobile NOMA Visible Light Communication System," 2019.

[28] M. Vaezi, Z. Ding, and H. V. Poor, *Multiple Access Techniques for 5G Wireless Networks and*. .

[29] H. Ren *et al.*, "Performance Improvement of M-QAM OFDM-NOMA Visible Light Communication Systems," *2018 IEEE Glob. Commun. Conf. GLOBECOM 2018 - Proc.*, pp. 1–6, 2018.

[30] B. Lin, X. Tang, and Z. Ghassemlooy, "Optical Power Domain NOMA for Visible Light Communications," *IEEE Wirel. Commun. Lett.*, vol. PP, p. 1, 2019.

[31] S. Dimitrov, S. Sinanovic, and H. Haas, "Clipping Noise in OFDM-based Optical Wireless Communication Systems," no. April, 2012.

[32] L. Yin, H. Haas, A. B. Introduction, and L. Communication, *Non-Orthogonal Multiple Access in LiFi Networks*. Springer International Publishing, 2019.

[33] H. Elgala, R. Mesleh, and H. Haas, "An LED Model for Intensity-Modulated Optical," vol. 22, no. 11, pp. 835–837, 2010.

[34] Z. H. Gebeyehu, "Heliyon Impact of clipping noise on the sum rate of NOMA with PD-DCO-OFDM and conventional DCO-OFDM," *Heliyon*, vol. 6, no. January, p. e03363, 2020.

[35] L. Yin, W. O. Popoola, X. Wu, and H. Haas, "Performance Evaluation of Non-Orthogonal Multiple Access in Visible Light Communication," 2016.

[36] L. Yin, W. O. Popoola, X. Wu, and H. Haas, "Performance Evaluation of Non-Orthogonal Multiple Access in Visible Light Communication," *IEEE Trans. Commun.*, vol. 64, no. 12, pp. 5162–5175, 2016.

[37] H. Jiang, Y. Wang, X. Yue, and X. Li, "Performance analysis of NOMA-based mobile edge computing with imperfect CSI," *Eurasip J. Wirel. Commun. Netw.*, vol. 2020, no. 1, 2020.

[38] L. Yin, W. O. Popoola, X. Wu, and H. Haas, "Performance Evaluation of Non-Orthogonal Multiple Access in Visible Light Communication," vol. 6778, no. c, pp. 1–15, 2016.

[39] M. Aldababsa, C. Goztepe, G. K. Kurt, and O. Kucur, "Bit error rate for NOMA network," *IEEE Commun. Lett.*, vol. 24, no. 6, pp. 1188–1191, 2020.

[40] S. Ali, H. Tabassum, and E. Hossain, "Dynamic User Clustering and Power Allocation for Uplink and Downlink Non-Orthogonal Multiple Access (NOMA) Systems," vol. 3536, no. c, pp. 1–18, 2016.

[41] K. M. Rabie, B. Adebisi, E. H. G. Yousif, H. Gacanin, and A. M. Tonello, "A Comparison between Orthogonal and Non-Orthogonal Multiple Access in Cooperative Relaying Power Line Communication Systems," *IEEE Access*, vol. 5, pp. 10118–10129, 2017.

[42] J. Song, T. Cao, and H. Zhang, "A low complexity NOMA scheme in VLC systems using pulse modulations (invited paper)," *2020 29th Wirel. Opt. Commun. Conf. WOCC 2020*, no. 2015, 2020.

[43] I. Hadj-kacem, H. Braham, and S. Ben Jemaa, "SINR and rate distributions for downlink cellular networks," vol. 1276, no. c, pp. 1–13, 2020.

[44] S. Ali, E. Hossain, and D. I. Kim, "Non-Orthogonal Multiple Access (NOMA) for Downlink Multiuser MIMO Systems : User Clustering , Beamforming , and Power

Allocation,” vol. 3536, no. c, pp. 1–13, 2016.

[45] Y. Fu, Y. Hong, L. K. Chen, and C. W. Sung, “Enhanced Power Allocation for Sum Rate Maximization in OFDM-NOMA VLC Systems,” *IEEE Photonics Technol. Lett.*, vol. 30, no. 13, pp. 1218–1221, 2018.

[46] S. Tao, H. Yu, Q. Li, and Y. Tang, “Performance analysis of gain ratio power allocation strategies for non-orthogonal multiple access in indoor visible light communication networks,” *Eurasip J. Wirel. Commun. Netw.*, vol. 2018, no. 1, 2018.

[47] J. A. Oviedo and H. R. Sadjadpour, “A new NOMA approach for fair power allocation,” *Proc. - IEEE INFOCOM*, vol. 2016-Septe, pp. 843–847, 2016.

[48] A. Adnan, Y. Liu, C. Chow, and C. Yeh, “Demonstration of non-Hermitian symmetry (NHS) IFFT / FFT Size Efficient OFDM Non-Orthogonal Multiple Access (NOMA) for Visible Light Communication,” pp. 3–7, 2020.

[49] T. Assaf, A. Al-Dweik, M. S. El Moursi, H. Zeineldin, and M. Al-Jarrah, “Exact Bit Error-Rate Analysis of Two-User NOMA Using QAM with Arbitrary Modulation Orders,” *IEEE Commun. Lett.*, pp. 1–1, 2020.

[50] T. Assaf, A. Al-Dweik, M. El Moursi, and H. Zeineldin, “Exact BER Performance Analysis for Downlink NOMA Systems over Nakagami-m Fading Channels,” *IEEE Access*, vol. 7, pp. 134539–134555, 2019.

[51] H. Haroyan, G. Hovsepyan, and S. Sargsyan, “Power Domain Non-orthogonal Multiple Access (PD-NOMA) Technique For 5G Networks,” vol. 11, no. 4, pp. 284–287, 2018.